water

MDPI

Article

Degradation of Dimethylacetamide from Membrane Production through Constructed Wetlands—Pathways, Ecotoxicological Effects and Consequences for Chemical Analysis

Thomas Schalk [1,*], Sara Schubert [2,3], Anja Rollberg [4], Dirk Freitag-Stechl [5], Annika Schubert [2], Alan Xavier Elena [2], Christian Koch [1] and Peter Krebs [1]

[1] Institute of Urban and Industrial Water Management, Technische Universität Dresden, 01062 Dresden, Germany
[2] Institute of Hydrobiology, Technische Universität Dresden, 01062 Dresden, Germany
[3] Institute of Clinical Pharmacology, Faculty of Medicine Carl Gustav Carus, Technische Universität Dresden, 01307 Dresden, Germany
[4] B. Braun Avitum Saxonia GmbH, 01454 Radeberg, Germany
[5] CUP Laboratorien Dr. Freitag GmbH, 01454 Radeberg, Germany
* Correspondence: thomas.schalk@tu-dresden.de

Abstract: Wastewater from factories producing polysulfone-based membranes mainly contains the used organic solvent, i.e., dimethylacetamide (DMAc). Due to the environmental impact of DMAc, wastewater treatment is mandatory. Several biological treatment options based on the activated sludge process are described in the literature. Due to artificial aeration, these techniques have high energy requirements. Near-nature processes such as vertical flow constructed wetlands (VF wetlands) have a low energy demand, high tolerance to load fluctuations, and low maintenance requirements. Therefore, high-loaded, two-stage VF wetlands are an efficient option for treating wastewater. However, constructed wetlands have so far only been used to a limited extent for the treatment of industrial wastewater. In the present study, the ability of laboratory-scale, high-load, two-stage VF wetlands to treat DMAc was investigated. This included their DMAc degradation efficiency and corresponding pathways, removal of the total organic carbon (TOC), nitrification and denitrification of the nitrogen, as well as the ecotoxicological effects (mutagenicity, genotoxicity, reactive oxygen species) of untreated and treated wastewater. The focus was to determine the effect of different grain size distributions on removal rates, the maximum inflow loading, and the effect of high inflow concentrations on effluent concentrations. In general, DMAc was completely degraded using VF wetlands, with dimethylamine (DMA) identified as the main intermediate. TOC removal rates reached more than 99%. The nitrogen bound to DMAc was completely nitrified. However, the start-up of the VF wetlands without seeded filter material temporarily leads to high nitrite accumulation. This may affect the mutagenicity of the treated wastewater. The results show that high-loaded, two-stage VF wetlands are an effective option for treating wastewater containing DMAc with higher efficiency than comparable biological processes.

Keywords: constructed wetlands; industrial wastewater treatment; membrane production; dimethylacetamide; ecotoxicological potential; microbial assay; nitrogen removal; theoretical oxygen demand

Citation: Schalk, T.; Schubert, S.; Rollberg, A.; Freitag-Stechl, D.; Schubert, A.; Elena, A.X.; Koch, C.; Krebs, P. Degradation of Dimethylacetamide from Membrane Production through Constructed Wetlands—Pathways, Ecotoxicological Effects and Consequences for Chemical Analysis. *Water* **2023**, *15*, 1463. https://doi.org/10.3390/w15081463

Academic Editors: Krzysztof Jóźwiakowski, Magda Kasprzyk and Piotr Bugajski

Received: 23 March 2023
Revised: 4 April 2023
Accepted: 6 April 2023
Published: 8 April 2023

1. Introduction

N,N-dimethylacetamide (DMAc), N,N-dimethylformamide (DMF), and N-methyl-2-pyrrolidone (NMP) are organic solvents commonly used for producing polysulfone-based membranes [1–4]. DMAc is classified as hazardous to health, e.g., by the European Chemicals Agency (ECHA) [5], and furthermore, as clearly hazardous to water by the German Environment Agency [6]. This underlines the need for treating DMAc-containing wastewater before discharge into a water body.

During membrane production, much of the DMAc can be recycled internally, for instance, by distillation [7], and can be reused. However, waste containing DMAc is generated that is not suitable for recycling.

Several approaches exist to remove DMAc from wastewater, including biological [8–11] and physicochemical treatment processes. Treatment processes considered include membrane treatment [12,13], sequencing batch reactors (SBR) [12,14,15], and bioelectric anaerobic systems [16]. Furthermore, Fenton [17–21] and electrochemical processes [22] are used as pretreatment [21] or as alternative techniques [20]. Studies dealing with biodegradation differ strongly in terms of load and operating conditions.

Aerobic biofilm processes, particularly moving bed biofilm reactors (MBBR) and vertical flow constructed wetlands (VF wetlands), provide alternative treatment options. Among these, VF wetlands provide huge potential due to their ability to remove organic substances at high rates, reliable nitrification performance [23–25], and high tolerance to load fluctuations [26,27]. VF wetlands have been demonstrated to be suitable for treating municipal and domestic wastewater [26,28,29] as well as wastewater from commercial bakeries, dairy farms, food processing, and the beverage industry [30–32]. Furthermore, VF wetlands were shown to efficiently treat wastewater containing chemical substances such as aromatic and nitro-aromatic compounds [33], hydrocarbons [34], methyl tertiary-butyl ether (MTBE), benzene [35], and dichloroethane [36]. VF wetlands are easier to establish than conventional aerobic treatment processes and have lower energy and maintenance requirements. In addition, nitrification can adapt to inhibitory substances [27]. Most of the named studies dealing with biological DMAc removal achieve an adequate [14,16] to very good [12,13] degradation efficiency but no or only partial nitrification; therefore, VF wetlands can be an alternative treatment process. Since they require more surface area, they are used when wastewater generation is low. For wider application in industrial wastewater treatment, the area required has, therefore, been reduced. Consequently, here, we performed a laboratory feasibility test for the use of VF wetlands for DMAc removal.

In Germany, municipal and domestic VF wetlands are designed according to the German standard DWA-A 262 [37,38]. However, no standards for industrial wastewater exist. Thus, it is necessary to conduct a test series to determine design parameters for the degradation of DMAc. To reduce the area required for a later treatment facility, here, a two-staged, high-loaded process was selected.

The aims of the research were to achieve the complete biodegradation of DMAc and complete nitrification of DMAc-bound nitrogen in combination with the low ecotoxicological potential of the resulting treated wastewater. This included the examination of removal rates for DMAc and TOC, nitrification rates, the effect of different grain size distributions on removal rates, maximum inflow loading, and the effect of high inflow concentrations on effluent concentrations. In addition, bioassays were carried out to investigate ecotoxicological effects. Test series were conducted with synthetic DMAc solutions and verified with real wastewater from a membrane-producing factory.

2. Materials and Methods

2.1. Test Setup

2.1.1. Lab-Scale Plants

Four lab-scale test plants were operated (I, II, III, IV). The test plants I and II were operated during the first test series, and plants III and IV during the second test series (Section 2.1.3). The first two plants consisted of one first stage and two second stages in parallel (Figure 1). Test plant I consisted of columns IA (first stage), IB (second stage), and IC (second stage); test plant II, columns IIA (first stage), IIB, and IIC (second stage). Four grain-size-distributions were researched (Table 1), which were based on the German standard DWA-A 262 [37,38] and our own pretrial experiences. The filter materials of the first stages differed; the materials of the second stages were equal between the test plants. The test plants III and IV were each operated with a first (IIIA, IVA) and a single second stage (IIIB, IVB). The first stages were filled with gravel (grain size 2–8 mm), and the second

stages with sand (grain size: 0–2 mm, Table 1). The columns of the plants were made of polyethylene, the pipes of stainless steel, and the suction tubes of PVDF. Timer-controlled diaphragm metering pumps (ProMinent GmbH, Germany; Emec S.r.l., Italy) were used to feed the columns. The first stages had a larger diameter to ensure the required volume for sampling and for the second stages. The filter materials originated from a gravel quarry near Dresden. Before it was used in the columns, it was washed and dried.

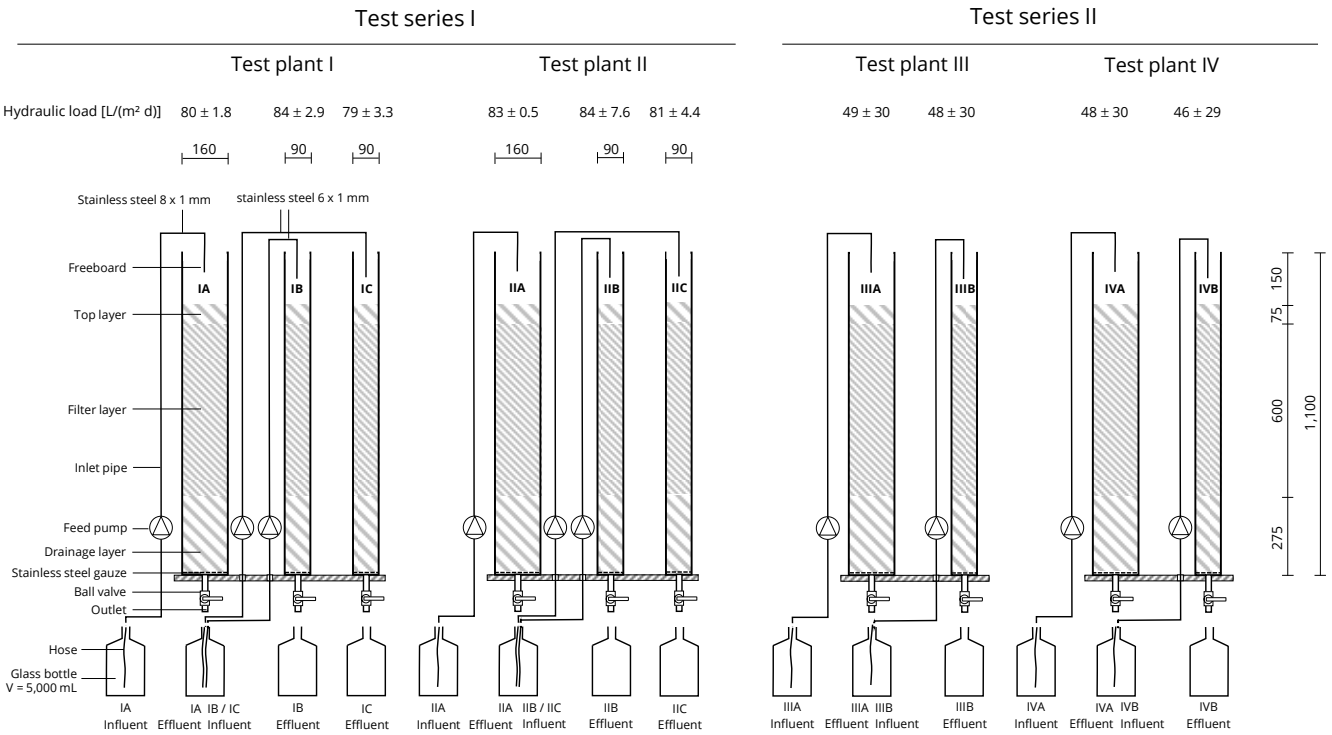

Figure 1. Setup of the test plants.

Table 1. Grain sizes of the columns used in the test plants.

Trial no.	Combination	1st Stage		2nd Stage		Feed
		Column	Grain Size	Column	Grain Size	
1	IA + IB	IA	2–4 mm	IB	0–2 mm	DMAc
	IA + IC	IA	2–4 mm	IC	2–4 mm	DMAc
	IIA + IIB	IIA	2–8 mm	IIB	0–2 mm	DMAc
	IIA + IIC	IIA	2–8 mm	IIC	2–4 mm	DMAc
2	IIIA + IIIB	IIIA	2–8 mm	IIIB	0–2 mm	Wastewater
	IVA + IVB	IVA	2–8 mm	IVB	0–2 mm	DMAc

2.1.2. Substrate Used

The tests of the second trial were conducted with synthetic wastewater and with real wastewater from a membrane-producing factory in parallel, while during the first trial, synthetic wastewater was exclusively used. A 2.5-% solution of N,N-dimethylacetamide (CAS: 127-19-5, Carl Roth GmbH + Co. KG, Karlsruhe, Germany) was used as a stock solution. The nutrient solution added to ensure biological degradation is based on ATV (1990) and was composed of $CuCl_2$ (0.22 g/L), $CoCl_2 \cdot 6H_2O$ (0.11 g/L), $ZnSO_4 \cdot 7H_2O$ (0.82 g/L), $MnCl_2 \cdot 4H_2O$ (0.24 g/L), $(NH_4)_6Mo_7O_{24} \cdot 4H_2O$ (0.11 g/L), $CrCl_3 \cdot 6H_2O$ (0.10 g/L), $NiSO_4 \cdot 7H_2O$ (0.14 g/L), $MgSO_4 \cdot 7H_2O$ (41 g/L), Se (1 g/L), $FeSO_4 \cdot 7H_2O$ (0.22 g/L). The nutrient solution was dosed proportional to the COD load (2 mL/g COD). KH_2PO_4 was added to ensure a COD:P ratio of 200:1. Later, the dosage was adjusted. As long as phosphate was detectable in excess in the effluent, the addition of phosphate was

reduced. Sodium bicarbonate was dosed as the carbon source according to the demand for complete nitrification. The wastewater used for feeding plant III was taken from a commercial plant operated by B. Braun Avitum Saxonia GmbH. The composition of the two wastewater samples taken is shown in Table 2. According to the DMAc concentrations needed, the wastewater was supplemented with DMAc stock solution.

Table 2. Wastewater composition from a membrane manufacturing factory.

Parameter	Unit	Charge 1	Charge 2
Dimethylacetamide (DMAc)	[mg/L]	2875	2287
Dimethylamine (DMA)	[mg/L]	274	143
Total organic carbon (TOC)	[mg/L]	1966	1408
Chemical oxygen demand (COD) [1]	[mg/L]	4789	3801
Total nitrogen (TNb)	[mg/L]	658	452
Ammonium nitrogen (NH_4-N)	[mg/L]	<3	<3

Note: [1] For reliability of COD values, see Section 4.9.

2.1.3. Test Series

Two test series were conducted. During the first series, different grain sizes and the impact of the load conditions on the removal rate were investigated. During the second trial, the DMAc- and the TOC-load were kept at a constant level, whereas the hydraulic load was decreased for studying the effect of the inflow concentration on the effluent concentration level. The last setup was equal to the expected load and hydraulic conditions of wastewater from a membrane production factory. To evaluate the impact of the influent concentrations on the effluent concentrations, the effluent values (Section 3.3) were grouped as a function of the influent concentration level (Section 3.1.2). The influence of the feed concentrations on nitrification was determined in a similar way. First, nitrogen balances were prepared (Section 2.3, Figure A4). Then, the ratio between the denitrified and the influent nitrogen loads was compared with the influent nitrogen concentration. The wastewater temperature averaged during the first test series was 22.3 ± 0.3 °C, and during the second, 22.6 ± 0.4 °C. The first test series lasted 23 weeks. The tests were conducted with a synthetic DMAc–nutrient mixture. All columns were operated with the same hydraulic load (mean values 79–84 L/(m^2 d), Figure 1). The test plants were operated without seeding. During the second test series, test plant III was fed with wastewater from a membrane manufacturing factory, and test plan IV with a synthetic DMAc solution. The test plants were operated with increasing wastewater concentrations and decreasing hydraulic load but a constant TOC load. To reduce the start-up time, the filter materials of the first test series were dried and mixed with new sand and gravel. The second test series lasted 28 weeks.

2.1.4. Operation and Sampling

The feed solutions were applied three times a week (Monday, Wednesday, and Friday). Feeding of the columns proceeded daily. The first stages were fed every 6 h, and the second stages every 12 h. During the second test series, the first stages were fed every 12 h during the first five weeks. Afterward, the interval changed to 6 h (see Section 3.3). Volume determination was performed three times a week by weighing the inlet and outlet quantity of each column. In parallel, samples were collected from the effluent of each stage. These samples were combined to obtain weekly composite samples.

2.2. Analytical Methods

2.2.1. Chemical Analyses

All samples were analyzed according to the German standard methods for the examination of water, wastewater, and sludge. The samples were analyzed for total organic carbon (TOC) and, after filtration through 0.45 µm membrane filters (Sartorius AG, Göttingen, Germany), for dissolved organic carbon (DOC) and inorganic dissolved carbon (IDC) according to the German standard DIN EN 1484 using a TOC-V CPH analyzer (Shimadzu

Deutschland GmbH, Duisburg, Germany). Furthermore, the total chemical oxygen demand (COD_{tot}, tube tests according to the German standard DIN ISO 15705–Hach Lange GmbH, Düsseldorf Germany), total suspended solids (TSS, German standard DIN 38409-2), total nitrogen (TNb, German standard DIN EN 12260 using a TOC-V CPH analyzer (Shimadzu Deutschland GmbH, Duisburg, Germany)), ammonium-nitrogen (NH_4-N, spectroquant 114752–Merck KGaA, Darmstadt Germany), the acid capacity (German standard DIN 38409-7 using a METROHM 888 Titrano, Deutsche Methrom GmbH and Co. KG, Filderstadt, Germany), and orthophosphate (oPO_4-P, spectroquant 114848–Merck KGaA, Darmstadt, Germany) were analyzed. Additionally, nitrate (NO_3-N, German standard DIN EN 38405-9) and nitrite nitrogen (NO_2-N, spectroquant 114776–Merck KGaA, Darmstadt, Germany) were quantified in the effluent samples. Since the oxygen demand of nitrite is included in COD analyses, the measured COD concentrations were corrected. DMAc was analyzed after filtration through 0.22 µm membrane filters (Macherey-Nagel™, Düren, Germany) with the HPLC method at B. Braun Avitum Saxonia laboratory (UltiMate 3000, Thermo Fisher Scientific Inc., Waltham, MA, USA). DMA measurements were conducted at CUP Laboratorien Dr. Freitag GmbH (CUP). The samples were analyzed after filtration through 0.45 µm membrane filters with the ion chromatography method using Ionenchromatograph 930 Compact IC Flex (Deutsche Methrom GmbH and Co. KG, Filderstadt, Germany). The method is based on the Ph. Eur. 2.2.29 "Liquid chromatography" and the Metrohm application note AW DE 8-0543-112004. Conductivity (WTW Multi 3620 DS with IDS® TetraCon® 925-3, Xylem Analytics Germany Sales GmbH and Co., Weilheim, Germany), temperature, and pH were measured daily in the fresh samples (WTW Multi 3620 DS with IDS® Sentix® 940-3, Xylem Analytics Germany Sales GmbH and Co., Weilheim, Germany).

2.2.2. Microbial Composition

The microbial composition was determined in test plants III and IV at the end of the test series. From the first stages, two composite samples each were taken from the upper filter section (0–300 mm filter height) and from the lower filter section (301–600 mm filter height). From the second stages, one composite sample each was taken. Samples were given to CUP Laboratorien Dr. Freitag GmbH for conducting microbial assays. Biochemical identification was not conducted for the entire spectrum but only for the major representatives that appeared when pure cultures were planted. The method used is based on the Ph. Eur 2.6.12 "Microbial examination of nonsterile products: Microbial enumeration tests", the Ph. Eur 2.6.13 "Microbial examination of nonsterile products: Tests for specified microorganisms", and on the German standard DIN EN ISO 7218:2014-09 "Microbiology of food and animal feeding stuffs-General requirements and guidance for microbiological examinations". From the samples taken, pure cultures were prepared with smear preparation. The cultures were evaluated according to macro-morphological criteria (color, profile, boundary, surface, and consistency), and after that, with microscopic examination. The Potassium Hydroxide Test was used to differentiate Gram-positive bacteria and Gram-negative bacteria. Furthermore, the cytochrome oxidase test using test strips and the catalase test using hydrogen peroxide (3%) were conducted. Finally, bacteria were classified with API (analytical profile index), MALDI-TOF (matrix-assisted laser desorption/ionization with time-of-flight mass spectrometer), and sequencing. All cultures were tested with the API test system. Results were evaluated using the internet database supplied by bioMérieux (https://apiweb.biomerieux.com, accessed on 12 November 2022). Strains that could not be classified with the API test system were classified using an external certified company using MALDI-TOF and sequencing.

2.2.3. Genomic Analysis of DMAc Degradation Pathways

To determine if identified bacteria were capable of complete or contribution to DMAc degradation, available reference genomes for the different isolated species recovered in this study were downloaded (*Brevibacillus non-reactive* GCA_900637055.1, *Brucella anthropi* GCA_012103185.1, *Chryseobacterium lacus* CA_003336205.1, and *Microbacterium oxydans*

GCA_003991855.1). Then, the Kyoto Encyclopaedia of Genomes and Genes (KEGG-https://www.genome.jp/kegg/, accessed on 12 January 2023) was accessed to query for genes encoding for enzymes involved in the different known microbial degradation pathways of DMAc (Table 3). Genes encoding for all steps of DMAc degradation, except for an enzyme that could directly metabolize DMAc into DMA, were identified. However, several enzymes involved in the production of DMA or similar compounds, as well as enzymes that cleave compounds similar to DMAc as substrate, were considered candidates (Table 3). The coding sequences of the identified strains' genomes were then thoroughly checked using BlastP to identify if the candidate enzymes or alternative enzymes providing similar biochemical functions included in DMAc degradation are present in the strains. For the missing cleavage of DMAc to DMA, a candidate protein involved in the glycine cleavage system (AN: WP_061347007.1) was found in the genome of *B. anthropi*, which shared the trimethylamine-oxide aldolase domain of the corresponding candidate enzyme. No crystallographic structures of this enzyme belonging to *B. anthropi* were deposited in the Protein Data Bank. Consequently, a proxy from *Shewanella massilia* [39] was downloaded and used for docking simulation to test if DMAc as a ligand can indeed dock to the active center of the protein for degradation. Polar hydrogens and atomic charges were assigned to both protein and ligand (DMAc) using AutoDock Tools V 1.5.7. The docking was carried out using AutoDock Vina V 1.2.0 [40,41]; modes were considered successful if they showed a root mean squared deviation of less than 2 Å and a negative affinity score.

Table 3. Genes encoding for enzymes and candidate enzymes involved in DMAc degradation.

Enzyme	EC [1]	Catalyzed Process
Methylphosphonate transferase	2.7.8.37	DMAc → DMA (Candidate gene)
Trimethylamine-oxide aldolase	4.1.2.32	DMAc → DMA (Candidate gene)
Dimethylamine/trimethylamine dehydrogenase	1.5.8.1	Dimethylamine (DMA) → Methylamine
Methylamine dehydrogenase heavy chain	1.4.9.1	Methylamine → Formaldehyde
Dimethylformamide amidohydrolase	3.5.1.56	DMAc → DMA (Candidate gene)
Acetyl-CoA-arylethylamine-N-acetyltransferase	2.3.1.87	Acetyl-Coa → N-acetyl-2-arylethylamine
Cytochrome P450 2E1	1.14.14.	Oxidative demethylation of DMAc
Acetate kinase	2.7.2.1	Acetate → Acetylphosphate
Acetyl-CoA synthase	6.2.1.1	Acetate → Acetyl-CoA
Succinyl-Coa:acetate CoA-transferase	2.8.3.18	Acetate → Acetyl-CoA
Acetaldehyde dehydrogenase	1.2.1.10	Acetaldehyde → Acetyl-CoA

Note: [1] Enzyme Commission Number.

2.2.4. In Vitro Bioassays

To test the (eco-)toxic potential of raw and treated wastewater, different in vitro bioassays were applied. (I) The Micronucleus test to measure genotoxic effects (induction of chromosome aberration or damage), (II) the ROS test to measure reactive oxygen species, and (III) the Ames fluctuation test to measure mutagenic effects (base-pair substitutions or frameshift mutations). Wastewater was tested in in vitro bioassays at three time points during treatment processes: in test plants I and II in weeks 11, 13, and 23 of operation and in test plants III and IV in weeks 4, 8, and 26. Wastewater was stored at −20 °C until testing. Defrosted samples were filtered through 0.22 µm syringe filters (TPP®, Trasadingen, Switzerland) and immediately used in the bioassays. For the Micronucleus test and ROS test, a cell line of human hepatocellular carcinoma (HepG2; German collection of Microorganism DSMZ, cell no. ACC-180, Braunschweig, Germany) was used and cultured in RPMI-1640 medium (with l-glutamine; ROTI®Cell RPMI-1640 CELLPURE®, Carl Roth GmbH + Co. KG, Karlsruhe, Germany) with 10% newborn calf serum (heat activated; Sigma-Aldrich, Taufkirchen, Germany) and 1% penicillin/streptomycin (WFI solution; Biochrom, Berlin, Germany) at 37 °C and 5% CO_2. HepG2 cells of passages 5 to 15 were used for both bioassays.

Micronucleus in vitro assay: For testing genotoxicity of raw and treated wastewater, the in vitro mammalian cell micronucleus test MNvit [ISO 21427-2; OECD TG 487] was conducted, and HepG2 cells were seeded ($6{\cdot}10^4$ cells/mL) onto adhesive microscope slides (Superfrost® UltraPlus by Menzel, Carl Roth GmbH + Co. KG, Karlsruhe, Germany) in four-well microtiter plates for an incubation period of 24 h [42,43]. Cells were then treated with three different dilutions of wastewater and in replicates for 24 h. The negative (medium) control was carried out in replicates using 5 mL culture medium only, and the positive control was carried out in replicates using 4 mL culture medium and 1 mL ethyl methanesulfonate (EMS, CAS 62-50-0, Sigma-Aldrich, Taufkirchen, Germany) at 1.75 mg EMS/mL in culture medium. After exposure for 24 h, treatment solutions were removed from each well, and 1.5% trisodium citrate (≥ 99%, Carl Roth GmbH + Co. KG, Karlsruhe, Germany) solution was added. Subsequently, cells were fixed twice using an iced solution of methanol:acetic acid:formaldehyde at 37% (3:1:0.05, v/v/v). After drying, slides were stained twice with 5% Giemsa solution for 15 and 20 min. The following solutions and compounds were used: methanol (purity > 99.8%, Carl Roth GmbH + Co. KG, Karlsruhe, Germany), glacial acetic acid (purity 100%, Carl Roth GmbH + Co. KG, Karlsruhe, Germany), formaldehyde solution (purity 37%, VWR International GmbH, Darmstadt, Germany), Giemsa stock solution (Carl Roth GmbH + Co. KG, Karlsruhe, Germany), and trisodium citrate. The analysis of MNvit was performed microscopically, and mono-, di-, tri- to tetra- and multi-nucleated cells as well as micronuclei per cell, were counted (Micronucleus rate, MNR). Approximately 500 cells per slide, two slides per dilution and control, as well as three different concentrations per wastewater sample, were counted; thus, approximately 1000 cells per control and 3000 cells per sample were analyzed.

ROS test (DCFH-DA assay): Intracellular ROS production (production of reactive oxygen species) was determined with 2′,7′-Dichlorfluorescein-diacetat (DCFH-DA, ≥97%, CAS 4091-99-0, Sigma-Aldrich, Taufkirchen, Germany) assay in microtiter plates (e.g., [44,45]) and modified in the following way for testing water (in cooperation with T. Grummt and M. Skerswetat, German Environment Agency, UBA Bad Elster, Germany): HepG2 cells were seeded into a 96-well-plate for fluorescence (µCLEAR®, Greiner Bio-One, Frickenhausen, Germany), cultured in RPMI medium (see MNvit assay) and covered by a breathable sealing film (Axygen®, VWR International GmbH, Darmstadt, Germany) for incubation of 24 h at 37 °C and 5% CO_2. For exposure, attached cells were washed twice with phosphate-buffered saline (PBS) to completely remove the serum-containing RPMI medium. Further, the cells were incubated with 40 µM DCFH-DA in serum- and phenol-red-free assay medium (ROTI®Cell RPMI-1640, Carl Roth GmbH + Co. KG, Karlsruhe, Germany) for 45 min at 37 °C and 5% CO_2 under dark conditions, afterward, washed twice with PBS to completely remove extracellular DCFH-DA and, then, exposed to wastewater at three different dilutions. The test was carried out with four replicates per sample and dilution and for each control. Blank controls (without cells) were conducted in eight replicates. For the negative control, cells were exposed to assay medium, and ultrapure water (Millipore® filter systems, Merck KGaA, Darmstadt, Germany) was used as dilution control since wastewater was diluted by ultrapure water. As positive controls, we used $PC_{SIN\text{-}1}$ with 1 mM SIN-1 (3-Morpholinosydnonimine hydrochloride, ≥98%, CAS 16142-27-1, Sigma-Aldrich, Taufkirchen, Germany) diluted in assay medium and, secondly, $PC_{SIN\text{-}1+Tiron}$ with 980 µM SIN-1 and 20 mM Tiron (4,5-Dihydroxy-1,3-benzenedisulfonic acid disodium salt monohydrate, 97%, CAS 270573-71-2, Sigma-Aldrich, Taufkirchen, Germany) diluted in assay medium [46–48]. After 4 h of exposure, fluorescence was measured (excitation of 485 nm, emission of 535 nm) using a microplate spectrophotometer from BioTek, Synergy H1 (now Agilent Technologies Deutschland GmbH, Germany). Additionally, external calibration curves of DCF (2′,7′-Dichlorfluorescein; ≥90%, CAS 76-54-0, Sigma-Aldrich, Taufkirchen, Germany) were performed in a standardized way with 8-point calibration curves and 4 replicates. Each ROS assay was accompanied by one external calibration curve.

Ames fluctuation test: The mutagenicity of wastewater samples was assessed using the Ames fluctuation test (ISO/CD 11350, OECD 471) with the *Salmonella typhimurium* strains TA98 (detection of frameshift mutation, hisD3052) and TA100 (detection of base-pair substitution, hisG46). The research group of J. Oehlmann (Department Aquatic Ecotoxicology, Goethe University Frankfurt am Main, Germany) kindly provided the used strains. Ames fluctuation tests were conducted as described by [49]. For testing native samples, overnight cultures were diluted to 1800 (TA98) and 450 (TA100) formazine attenuation units in the assay medium. The positive control was carried out using 4-Nitro-Phenylenediamine (4-NOPD, CAS 99-56-9, Sigma-Aldrich, Taufkirchen, Germany) for TA98 and nitrofurantoin (NF, CAS 67-20-9, Sigma-Aldrich, Taufkirchen, Germany) for TA100. Ultrapure water (Millipore® filter systems) was used for the dilution of wastewater. Three dilutions of samples were tested (80%, 40%, and 20% wastewater) in each strain. After an incubation of 48 h in 384-well plates, absorbance was measured (420 nm) using a microplate spectrophotometer.

2.3. Balancing

TOC was used for balancing because COD determination of DMAc and DMA leads to incorrect results (see Section 4.9). COD is only used for the inflow load. In this case, COD is calculated based on the DMAc load. The TOC removal rate was calculated according to Equation (1). The calculation of the DMAc removal rate and the DMA removal rate was performed analogously.

$$TOC_{rem} = TOC_{feed} - TOC_{eff} \quad (1)$$

TOC_{rem} is the removed TOC in g/(m^2 d); TOC_{feed} is the feed TOC content in g/(m^2 d); TOC_{eff} is the effluent TOC content in g/(m^2 d).

Nitrification and denitrification were calculated according to Equations (2) and (3).

$$N_{ni} = (TNb_{feed} - NO_3\text{-}N_{feed} - NO_2\text{-}N_{feed}) - N_{BM} - N_{org,eff} - NH_4\text{-}N_{eff} \quad (2)$$

N_{ni} is the nitrified nitrogen in g/(m^2 d); TNb_{feed} is the total nitrogen content of the feed in g/(m^2 d); $NO_3\text{-}N_{feed}$ is the feed NO_3-N content in g/(m^2 d); $NO_2\text{-}N_{feed}$ is the feed NO_2-N content in g/(m^2 d); N_{BM} is the biomass nitrogen demand in g/(m^2 d) (Equation (5)); $NH_4\text{-}N_{eff}$ is the effluent NH_4-N content in g/(m^2 d); $N_{org,eff}$ is the effluent organic nitrogen content in g/(m^2 d) (Equation (6)).

$$N_{deni} = (N_{ni} + NO_3\text{-}N_{feed} + NO_2\text{-}N_{feed}) - (NO_3\text{-}N_{eff} + NO_2\text{-}N_{eff}) \quad (3)$$

N_{deni} is the denitrified nitrogen in g/(m^2 d); N_{ni} is the nitrified nitrogen in g/(m^2 d) (Equation (2)); $NO_3\text{-}N_{feed}$ is the feed NO_3-N content in g/(m^2 d); $NO_2\text{-}N_{feed}$ is the feed NO_2-N content in g/(m^2 d); $NO_3\text{-}N_{effl}$ is the effluent NO_3-N content in g/(m^2 d); $NO_2\text{-}N_{eff}$ is the effluent NO_2-N content in g/(m^2 d).

Nitrogen balancing was verified by bicarbonate balancing (Equation (4)). Bicarbonate balancing was used for the determination of biomass nitrogen uptake. Bicarbonate balancing encloses nitrification bicarbonate demand, which contains the biomass nitrogen demand again.

$$HCO_{3,eff} = HCO_{3,feed} + (HCO_{3,DMAc,rem} + HCO_{3,DMA,feed} - HCO_{3,DMA,eff}) - (HCO_{3,ni} - HCO_{3,deni}) \quad (4)$$

$HCO_{3,eff}$ is the HCO_3 content of the effluent in mol/(m^2 d); $HCO_{3,feed}$ is the HCO_3 content of the feed in mol/(m^2 d); $HCO_{3,DMAc,rem}$ is the HCO_3 formation while DMAc removal in mol/(m^2 d) (1 mol HCO_3/mol $DMAc_{rem}$); $HCO_{3,DMA,feed}$ is the HCO_3 formation capability of the feed DMA in mol/(m^2 d) (1 mol HCO_3/mol DMA); $HCO_{3,DMA,eff}$ is the HCO_3 formation capability of the effluent DMA in mol/(m^2 d) (1 mol HCO_3/mol DMA); $HCO_{3,ni}$ is the HCO_3 demand for nitrification in mol/(m^2 d) (2 mol HCO_3/mol $N_{nitrified}$); $HCO_{3,deni}$ is the HCO_3 formation while denitrification in mol/(m^2 d) (1 mol HCO_3/mol $N_{denitrified}$).

The factor for biomass nitrogen demand (Equation (5)) was determined in an iterative way. The factor was adjusted until the slope of the linear regression between the measured and calculated bicarbonate effluent concentrations reached 1.0 for each column.

$$N_{BM} = 0.01 \cdot TOC_{rem} \quad (5)$$

N_{BM} is the biomass nitrogen demand in g/(m^2 d); TOC_{rem} is the removed TOC in g/(m^2 d).

The content of organic nitrogen was calculated according to Equation (6).

$$N_{org,eff} = TNb_{eff,unfilt} - NO_3\text{-}N_{eff} - NO_2\text{-}N_{eff} - NH_4\text{-}N_{eff} \quad (6)$$

$N_{org.eff}$ is the effluent organic nitrogen content in g/(m^2 d); $TNb_{eff,unfilt}$ is the effluent TNb content of the unfiltered sample in g/(m^2 d); NO_3-N_{eff} is the effluent NO_3-N content in g/(m^2 d); NO_2-N_{eff} is the effluent NO_2-N content in g/(m^2 d); NH_4-N_{eff} is the effluent NH_4-N content in g/(m^2 d).

The nitrifiable nitrogen is the nitrogen inflow corrected for biomass nitrogen demand according to Equation (7).

$$N_{nifia} = N_{DMAc,in} - N_{BM} \quad (7)$$

N_{nifia} is the nitrifiable nitrogen in g/(m^2 d); $N_{DAMc,in}$ is the nitrogen content of the DMAc inflow in g/(m^2 d); N_{BM} is the biomass nitrogen demand in g/(m^2 d).

2.4. Data Analysis

Ecotoxicological effects were leveled in no, moderate, or high toxic effects for each bioassay. Genotoxic effects (MNvit test) are leveled as follows: highly genotoxic effects were found in wastewater (ww) samples compared to positive controls (pc) with MNR_{ww} (in all/three dilutions) > MNR_{pc}, moderate genotoxic effects when MNR_{ww} (in 1 to 2 dilutions) > MNR_{pc} and no genotoxic effects were detected when $MNR_{ww} \leq MNR_{pc}$. The oxidative stress (ROS test) in wastewater was graded by comparison of fluorescence levels to both positive controls ($PC_{SIN\text{-}1}$, $PC_{SIN\text{-}1+Tiron}$): no oxidative stress when <$PC_{SIN\text{-}1}$, moderate oxidative stress when > $PC_{SIN\text{-}1}$, and high oxidative stress when >$PC_{SIN\text{-}1+Tiron}$. Mutagenic effects (Ames test) were graded in moderate effects when >20.8% of wells were affected and highly mutagenic when >41.6% of wells were affected.

3. Results

3.1. Inflow Load

3.1.1. First Test Series

The trials started with a load of 160 g COD/(m^2 d) and 48 g TOC/(m^2 d), respectively. After 12 weeks, the load was gradually increased to over 300 g COD/(m^2 d) (Figure 2). During the test, the hydraulic load was constant at 80 ± 1.8 L/(m^2 d) in column IA and at 83 ± 0.5 L/(m^2 d) in column IIA. When the performance limit of column IA was exceeded, the test series was stopped. In the whole test period, the COD inflow load averaged 204 ± 51 g/(m^2 d) in column IA and 211 ± 53 g/(m^2 d) in column IIA (Table A1). The difference between both columns was low and reached approximately 3%. Dependent on the DMAc inflow load, the nitrogen load was between 14 and 28 g/(m^2 d). The DMAc inflow concentrations were between 1.1 and 2.1 g/L. This is equivalent to 2.1 and 3.9 g COD/L. According to the DMAc concentration, the nitrogen concentration ranged from 180 to 340 mg/L (Figure 3, Table A1).

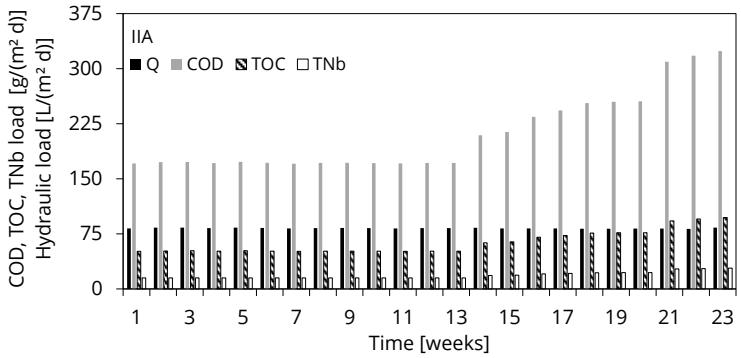

Figure 2. Load increase of the first stage during the first test series using the example of column IIA.

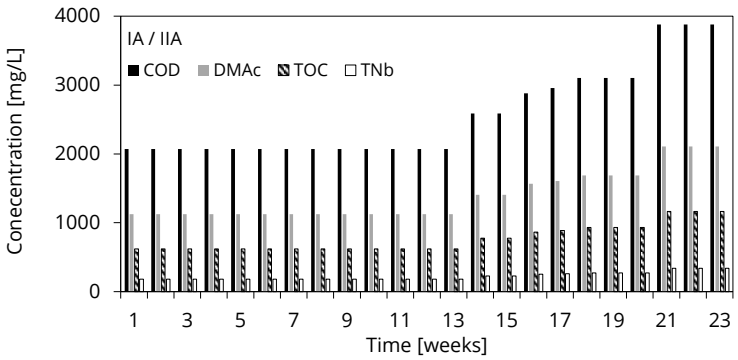

Figure 3. Concentrations of the inflow in the first stage during the first test series.

3.1.2. Second Test Series

The TOC inflow load averaged in columns IIIA and IVA 47 ± 2.1 g/(m^2 d) each (Table A2). The inflow load is equivalent to a COD load of approximately 160 g/(m^2 d). The hydraulic load decreased from 80 L/(m^2 d) gradually to 60, 30, 20, and 11 L/(m^2 d). In parallel, the TOC inflow concentration increased from 0.6 g/L up to 4.4 g/L (Figure 4). Due to differing inflow compositions of column IIIA (real wastewater) and IVA (synthetic wastewater), the load conditions differed slightly (Table A2). The differences result from substances contained in the real wastewater but not in the synthetic wastewater, e.g., acidic acid and DMA resulting from the decomposition of DMAc, as well as residues of the primary materials polyvinylpyrrolidone and polysulfone. The DMAc load averaged in column IIIA 75 ± 6.8 g/(m^2 d), and in column IVA 86 ± 3.8 g/(m^2 d). The nitrogen load was 15.1 ± 1.1 g/(m^2 d) in column IIIA and 13.8 ± 0.6 g/(m^2 d) in column IVA. The DMA load averaged in column IIIA 4.5 ± 2.4 g/(m^2 d). The feed of column IVA did not contain DMA.

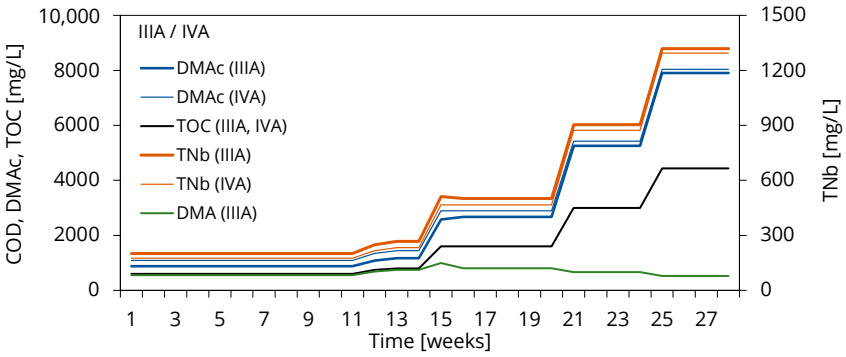

Figure 4. Concentrations of the inflow in the first stage during the second test series.

3.2. Results of the First Test Series

TOC removal: Neglecting the start-up phase, the TOC removal rate averaged 97–98% for all combinations (Figure 5a,b, Table A1). Temporarily, more than 99% of the TOC load was removed. The main part of the TOC load was removed in the first stages of the test plants (Figure 5c,d). The TOC effluent concentrations of the second stages did not differ much and decreased over time to less than 10 mg/L. In contrast, the first stages differed distinctly. The removal rate of column IA was worse than that of column IIA (Figure 5c,d, Table A1). Independent of loading conditions, the TOC concentrations in column IIA effluent remained under 30 mg/L after 12 weeks (Figure 6c). In column IA, the TOC effluent concentrations were between 54 and 84 mg/L. Due to the increasing load to more than 300 g COD/(m^2 d), TOC effluent concentrations of column IA increased to 148–181 mg/L. In contrast, the effluent concentrations of column IIA remained at a constant level.

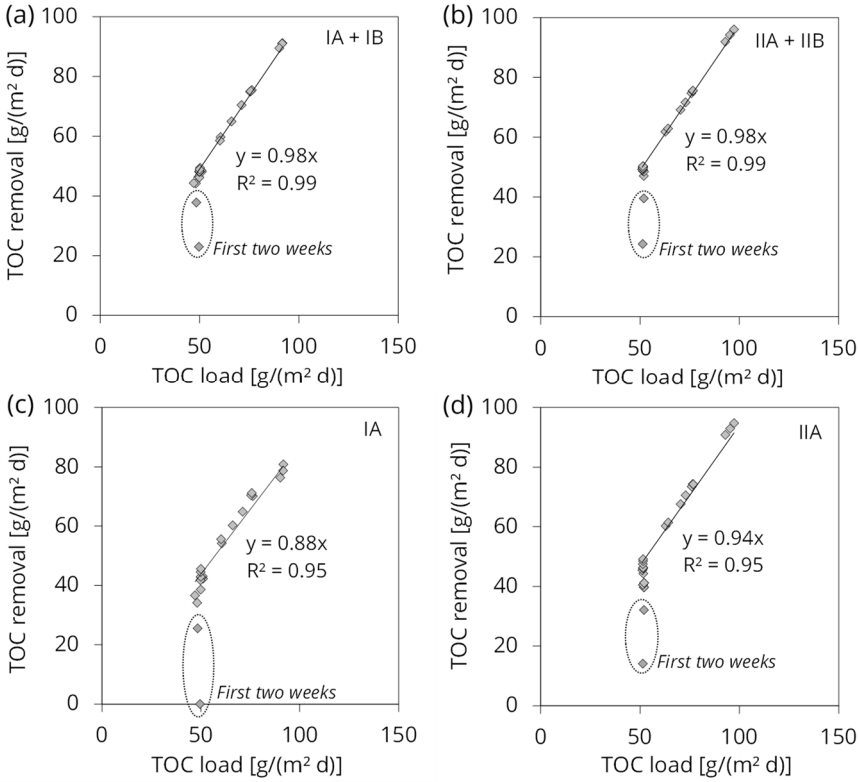

Figure 5. TOC removal efficiency of the combinations IA + IB (**a**), IIA + IIB (**b**), and of the first stages IA (**c**), IIA (**d**) during the first test series.

DMAc removal: In the effluent of the second stages, both DMAc and DMA were detectable for two weeks (Figure 6a,b). Afterward, the concentrations were below the limit of quantification (LOQ_{DMAc} = 0.1 mg/L, LOQ_{DMA} = 5 mg/L). In the effluent of the first stages, both DMAc and DMA were detectable for a much longer period, especially in column IA. One week after start-up, the DMAc concentration in the column IA effluent was equal to the inflow concentration. In column IIA, degradation processes did start. Thereby, DMA, an intermediate of DMAc degradation [13], was detected. First, the DMA concentrations increased in column IA over the following weeks before reaching a stable level below 100 mg/L, neglecting the last three weeks. In contrast to column IA, DMA was completely degraded after 12 weeks in column IIA (DMA < 5 mg/L). The differences during DMAc and DMA degradation correspond with those of TOC removal (Figure 6c). At the end of the trial, loading was increased to > 300 g COD/(m^2 d). This led to increasing DMAc concentrations in both first stages and, additionally, to significantly increasing DMA

concentrations in IB. Compared to column IA (C_{DMAc} = 7.4 mg/L), the DMAc increase was less in column IIA (C_{DMAc} < 1 mg/L).

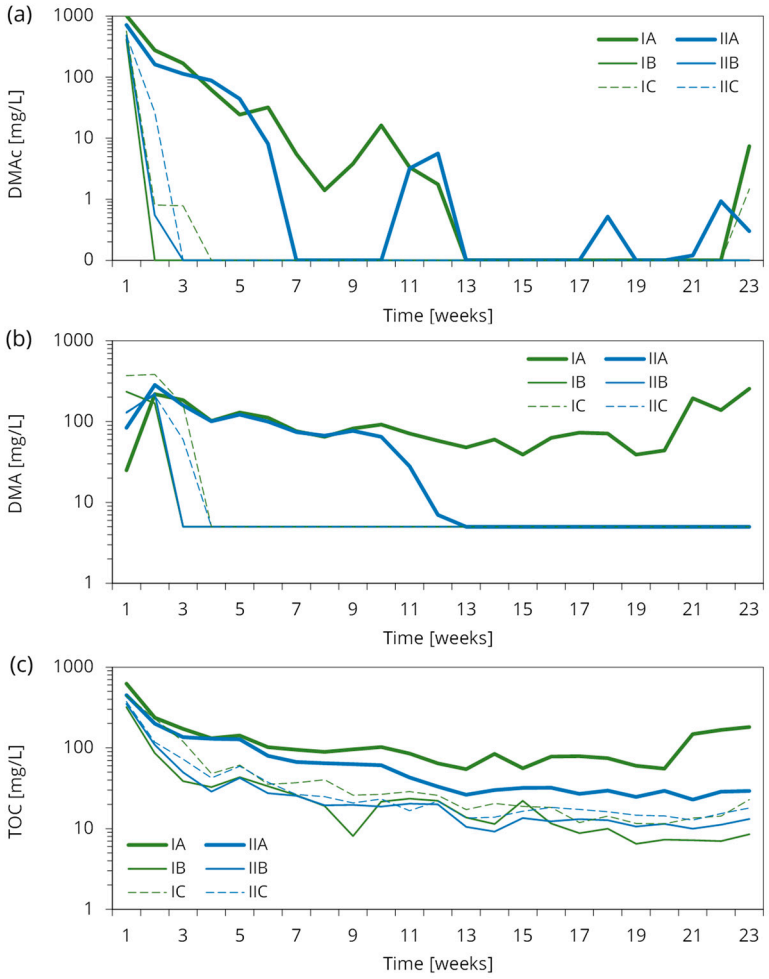

Figure 6. DMAc (**a**), DMA (**b**), and TOC (**c**) effluent concentrations during the first test series.

Nitrogen removal: The averaged NH_4-N effluent concentration was considerably higher in column IA at 80 ± 31 mg/L than in IIA at 26 ± 35 mg/L (Table A1). In IIA, the NH_4-N concentrations dropped gradually until below 3 mg/L, while in IA, they remained above 57 mg/L (Figure A1a). In the second stages, it took 7 weeks (IIB) and 8 weeks (IB, IIC) for NH_4-N concentrations to be below 10 mg/L. In the following weeks, the NH_4-N concentrations averaged at 3.5 ± 1.1 (IIB) and 3.7 ± 1.6 mg/L (IB, IIC). In the case of IC, it took several weeks longer for the NH_4-N concentration to reach below 10 mg/L. In addition, the average concentration was higher (6.9 ± 3.7 mg/L) than in the other columns.

When nitrification started, nitrite accumulated (Figure A1b). The maximum NO_2-N level was significantly higher in IIA at 100 mg/L compared to IA at 8 mg/L. NO_2-N accumulation reached in the second stages temporarily peak values at 142 mg/L. In columns IB and IIB, NO_2-N concentrations later stabilized at < 0.1 mg/L. In IIC, the values were slightly higher at < 0.2 mg/L (last 10 weeks). In IC, the NO_2-N concentration was considerably higher on average at 7.9 ± 9.2 mg/L (last 10 weeks). Nitrite build-up started simultaneously in columns IB, IIA, IIB, and IIC, whereby IA affected the following columns IIB and IIC by NO_2-N discharge. Despite no NO_2-N carryover occurring in IB, nitrite build-up began at the same time. Due to the low nitrite build-up in IA, nitrate formation was low, too. The nitrate concentrations were below 2 mg NO_3-N/L at all times. In comparison, the NO_3-N concentrations increased up to 100 mg/L in IIA and up to 115 mg/L in IB, IIB, and IIC (Figure A1c). Only in IC, nitrate formation was significantly lower. Decreasing TNb

concentrations indicate denitrification processes taking place (Figure A1d). Increased TNb concentrations in test plant I are due to a reduced nitrification rate in the first stage.

Although no nitrate and only temporary nitrite were detectable in IA effluent, the nitrification balance shows that nitrification is occurring in IA, but nitrate has been almost completely denitrified (Figure A2a, Table A1). Denitrification rates of columns IA and IIA are comparable, but in IIA, DMAc-bounded nitrogen was completely nitrified (Figure A2b). In the second stages, denitrification processes were low, so the overall efficiency was hardly influenced (Figure A2c,d). With the exception of the IA + IC combination, all other combinations reached nitrification rates of 80% (Figure A2c,d). Considering the biomass nitrogen demand (see Equation (7)), DMAc-bounded nitrogen has been completely nitrified (Table A1).

Due to sodium bicarbonate dosage to ensure nitrification, the effluent acid capacity was relatively high. The mean values over the last ten weeks ranged from 8.0 ± 2.9 mmol/L (IIB) and 8.0 ± 2.8 mmol/L (IIC) to 9.1 ± 2.5 mmol/L (IB) and 10.1 ± 2.3 mmol/L (IC). As a result, the pH was also high. The pH in the inflow averaged 8.7 ± 0.3. In the effluent of the first stages, pH decreased slightly to 8.5 ± 0.2 (IA, IB). In the effluent of the second stages, pH was slightly higher than the values in the influent and ranged from 8.8 ± 0.1 (IB) and 8.8 ± 0.2 (IC) to 8.9 ± 0.2 (IIB) and 9.0 ± 0.2 (IIC).

Ecotoxicological effects: Genotoxic effects, reactive oxygen species formation, and mutagenic effects were measured with in vitro bioassays at different time points during wastewater treatment. The initial influent of the first test series (test plants I and II) containing 1125 mg/L DMAc showed moderate genotoxic effects, no mutagenic effects in both strains (TA98 and TA100), and highly toxic effects in ROS formation. Figure 7 shows ecotoxicological effects in test plant I and II during the treatment period of 23 weeks measured after treatment weeks 11, 13, and 23. Stage 2 of both test plants were equipped with two different grain sizes (0–2 mm or 0–4 mm), and their effluents were also tested separately in the bioassays. To simplify the graphs, the results of test plant I and II are shown in their respective stages 2 as one result; if they differ from the result, the more toxic one is shown in the figure and exactly described in the following subchapter.

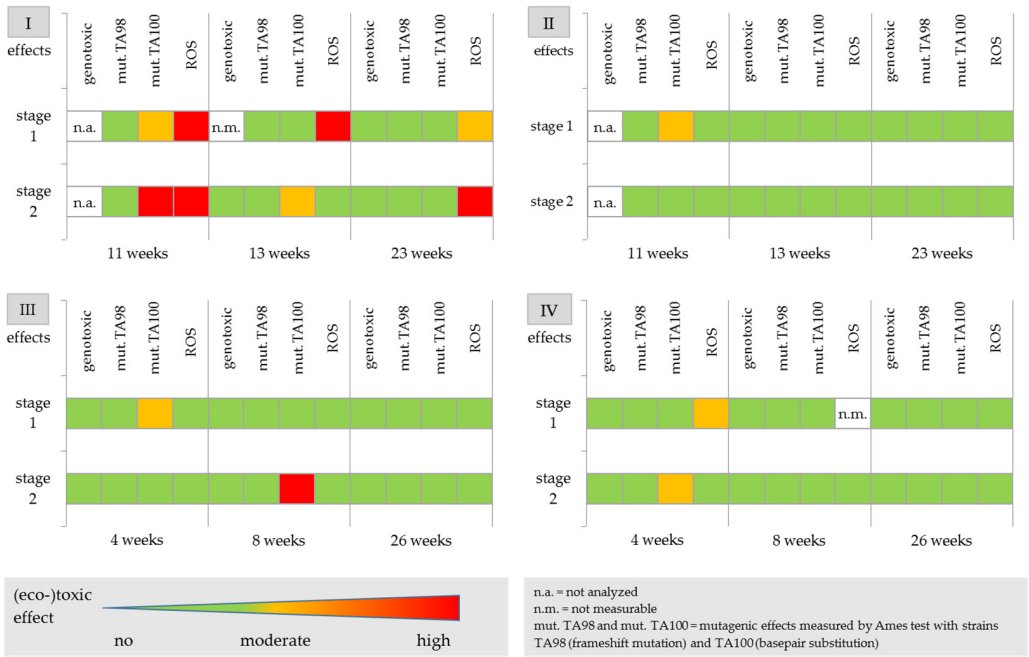

Figure 7. Ecotoxicological effects of the first test series (test plant **I** and **II**) and of the second test series (test plant **III** and **IV**). Detailed definitions of no, moderate, and high toxic effects for each biotest are described in the Methods section.

Regarding ecotoxicological effects of test plant I after 11 weeks of operation: mutagenic effects were detected for basepair substitution (strain TA100) at a moderate level in the effluent of stage 1 and at a high level in the effluent of stage 2 (grain size 0–2 mm: moderate; grain size 0–4 mm: highly toxic), further, ROS formation was detected in both stages. After 13 weeks of plant I operation, mutagenic effects were just found in stage 2 at a moderate level (TA100), and ROS formation was detected just in the effluent of stage 1. After 23 weeks of plant I operation, no genotoxic and no mutagenic effects, but ROS formation in stage 1 at a moderate level and in stage 2 at a high toxic level were identified. In summary, in plant I after 23 weeks of operation, genotoxic effects from the initial influent were successfully removed and mutagenic effects (TA100) detected during the treatment process were no longer detected. In contrast, ROS formation was still detected in the final effluent at similar levels to the initial influent of plant I.

In test plant II, a mutagenic effect (TA100) was found at a moderate level in stage 1 after 11 weeks of operation. Besides this single effect, no additional effects were found at 11, 13, and 23 weeks of operation. Therefore, the ecotoxicological effects of the initial influent could be removed after short-term operation time, and, compared to plant I, plant II was more efficient in terms of ecotoxicological effects.

3.3. Results of the Second Test Series

TOC removal: The TOC overall removal efficiency of test plants III and IV was above 95% (Table A2). During the test period, the efficiency averaged more than 99% (Figure 8a,b). In the first stages, it took more time until the TOC removal rate was stable compared to the first test series because the test plants were fed during the first five weeks only twice a day instead of four times a day (Figure 8c,d). After the alteration of the feeding times, the removal rates of the first stages increased. This implies that the load per feed cycle was too high. Independently, the effluent load of the first stages was removed in the second stages. As a result, the overall removal rate remained constant.

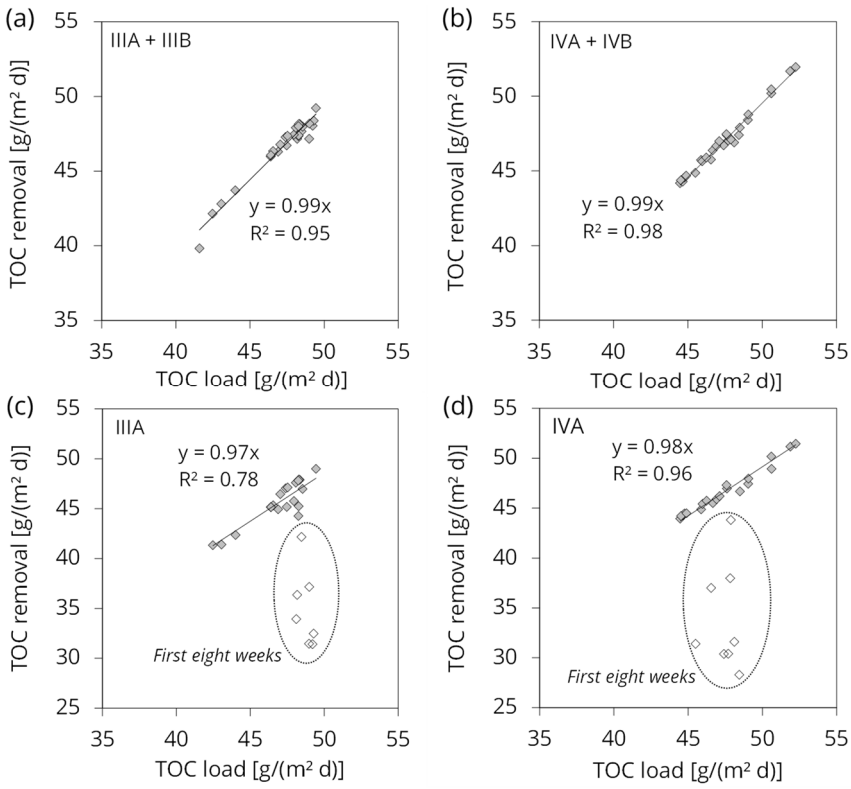

Figure 8. TOC removal efficiency of the combinations IIIA + IIIB (**a**), IVA + IVB (**b**), and of the first stages IIIA (**c**), IVA (**d**) during the second test series.

The TOC effluent concentrations were 10% lower when artificial wastewater than when real wastewater was treated (Figure 9c). The TOC effluent concentrations averaged 10.6 ± 6.4 mg/L for treating the artificial wastewater and 12.0 ± 4.2 mg/L for the real wastewater. The DMAc inflow concentrations influenced the effluent TOC concentrations (see Section 4.5).

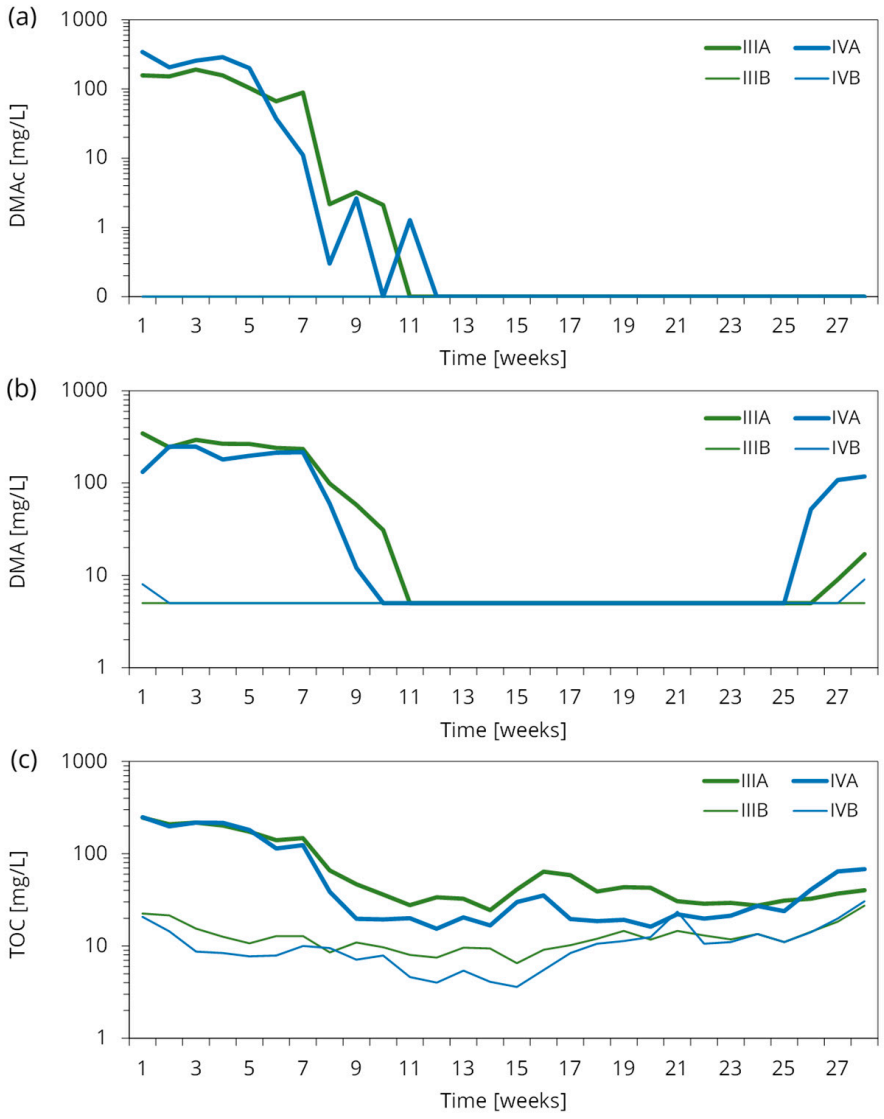

Figure 9. DMAc (**a**), DMA (**b**), and TOC (**c**) effluent concentrations during the second test series.

DMAc removal: DMAc was not detectable in the effluent of the second stages (Figure 9a, Table A2). DMA was only detected during the first week in test plant IV (8 mg/L, Figure 9b). In the first stages effluents, higher concentrations of DMAC, as well as DMA, were detected. The concentrations only decreased below the limit of quantification after feeding times were altered.

Nitrogen removal: Overall nitrification and denitrification rates were comparable for artificial and real wastewater treatment (Figure A4a–d). In the first stages, the removal rates differed temporarily. Although test plant IV was 10% less loaded than test plant III, the nitrification rate was lower at times (Figure A4b,d). Two weeks after start-up, NH_4-N concentrations dropped in the second stages effluent below 10 mg/L (Figure A3a).

In the first stages, the NH_4-N concentrations also decreased after adjusting feeding cycles (Figure A3a). In the last three weeks, the effluent NH_4-N concentrations from the first stage of test plant IV increased. The second stage was not affected.

Effluent NO_2-N concentrations were low at 0.2 mg/L (Figure A3b). The NO_3-N concentrations averaged 197 ± 140 mg/L (III) and 182 ± 107 mg/L (IV) (Table A2). Dependent on the inflow load, the nitrate concentrations peaked at 455 mg NO_3-N/L (Figure A3c). Nitrification was complete three weeks after start-up. Denitrification rates differed between test plants. Test plant III had a higher denitrification rate, averaging 7.0 g ± 1.4 $N_{DN}/(m^2\ d)$, than test plant IV, which averaged 6.0 ± 2.1 g $N_{DN}/(m^2\ d)$. The denitrification rates averaged 46 ± 10% in test plant III and 43 ± 14% in test plant IV (Figure A4a–d). During the test series, the denitrification and TNb removal rates varied (Figure A3d).

The NH_4-N concentration affects the adsorption of NH_4-N to the filter material [50–52]. When inflow NH_4-N concentration increases, a part of ammonia is adsorbed to the filter material; if NH_4-N content decreases, a part of the NH_4-N bound in the filter material is released. In the nitrogen balance, adsorption is summarized with denitrification (see Section 2.3). Thus, if NH_4-N is adsorbed, denitrification seems to increase. However, there was indeed an increase in the denitrification rate during the last three weeks in test plant IV (see Section 4.5).

Acid capacity averaged 9.4 ± 4.4 mmol/L in the effluent of IIIB and 8.2 ± 6.8 mmol/L in the effluent of IVB. In the inflow, pH averaged 8.5 ± 0.5 in test plant III and 8.3 ± 0.5 in test plant IV. In the effluent of the first stages, pH values changed slightly (IIIA: 8.3 ± 0.6, IVA: 8.4 ± 0.5). In the second stages effluent, the average pH values were higher than the influent values (IIIB: 8.9 ± 0.2, IVB: 8.8 ± 0.5).

Ecotoxicological effects: Wastewater of plants III and IV were tested in in vitro bioassays at weeks 4, 8, and 26 during the treatment process. Ecotoxicological effects were sporadic in test plants III and IV during the treatment period of 26 weeks (Figure 7). In test plant III, mutagenic effects (TA100) were found in the sample of 4 weeks of operation in stage 1 in moderate levels but not in stage 2. After 8 weeks of operation, mutagenicity (TA100) was detected in stage 2 at a high toxicity level. In the final effluent after 26 weeks of operation, no toxicity was detected in both stages. In plant IV after 4 weeks of operation, moderate mutagenicity (TA100) could be detected in stage 2, and moderate formation of ROS was found in stage 1 but not in stage 2. After 8 and 26 weeks run, no ecotoxicological effects were detected.

4. Discussion

4.1. Effect of the Grain Size Distribution on the Removal Rate

For the discussion, the last 10 weeks when TOC and nitrogen removal rates were stable were considered. The total removal rates of the combinations IA + IB, IIA + IIB, and IIA + IIC are comparable. Only the effluent concentrations show slight differences. The lowest TOC and NH_4-N effluent concentrations were observed for the combination IA + IB. In addition, this combination has the second-highest denitrification rate. In combination IIA + IIB, the TOC and NO_3-N effluent concentrations were higher than in IA + IB. This was followed by the combinations IIA + IIC and IA + IC. In general, sand (0–2 mm) showed better performance as a filter material in the second stages than fine gravel (2–4 mm). The different removal rates of the first stages were buffered by the second stages when sand was used. High load periods were also compensated without loss of removal efficiency. In contrast, clear differences in performance were observed between the first stages. In particular, the results of column IA indicate overload times. In the first stage, the material with a grain size of 2–8 mm (IIA) was more suitable than the material with a grain size of 2–4 mm (IA). In both cases, oxygen-limited zones occurred. These zones were larger in IA than in IIA. Due to the lower TOC removal and nitrate built up in column IA, the oxygen supply to column IA was probably weaker than to the coarser material of column IIA. While oxygen concentrations were not measured in the columns, the performance parameters endorse this conclusion.

Nitrogen balances indicate nitrification processes taking place in IA. However, the nitrate formed was completely consumed for the oxidation of DMAc and DMA, respectively. Since in column IA, the supply of dissolved oxygen and nitrate could not compensate

for the oxygen demand of the fed organic load, the TOC load in the effluent was higher than in column IIA. Due to incomplete denitrification of the nitrate formed in column IIA, it is proven that readily degradable TOC has been largely removed and that IIA is not overloaded. The lower TOC removal rate of IA was compensated by the second stage, but it is not useful to overload the first stage permanently. If oxygen-restricted conditions occur in aerobic systems, the formation of extracellular polymeric substances (EPS) may increase [53]. Under these conditions, so-called microaerophilic conditions, oxygen is available for the degradation of organic substances but not in sufficient quantities to degrade EPS formed during the degradation process [54]. Independently, high organic loading also results in high biomass growth and increasing EPS formation. Both can increase the risk for colmation [55–57]. As a result, the reliability of column IA is rated lower compared to IIA. Hence, a grain size of 2–8 mm should be used in the first stage.

4.2. Effect of the pH Value on the Removal Rate

In the effluent of the columns, the pH values reached a high level between 8.0 and more than 9.5. Favorable pH values for DMAc biodegradation are between 6 and 7 [8]. However, no significant negative effect on the removal rate was determined during the experiments.

4.3. Maximum Loading

The first stage loading was twice that of comparable two-stage municipal VF wetlands [37,38]. Nevertheless, the best-rated combination (IIA + IIB) was suitable for treating high loads of up to 300 g COD/(m^2 d) and 97 g TOC/(m^2 d) without affecting efficiency. The highest TOC load removed from the first stage was 95 g/(m^2 d) and 96 g TOC/(m^2 d) of the overall system. The highest total DMAc removal was 196 g/(m^2 d). Nitrification reached up to 25 g N/(m^2 d). Denitrification increased dependent on the DMAc load, up to 16 g N/(m^2 d).

In summary, the loading was relatively high compared to municipal VF wetlands. However, VF wetlands fed with industrial wastewater can be similarly loaded. For instance, [31] consider a two-stage system treating wastewater from food processing that has been loaded with 240 g COD/(m^2 d). Generalizable data are not available because several factors affect the safe loading of a VF wetland, e.g., biodegradability, wastewater composition, wetland type, especially setup and materials used, and wetland operating mode. For comparison, the design load of the first stage of the two-stage French wetland system is 300 g COD/(m^2 d) [37,38,58]. That is similar to the highest treated load of the trials carried out. However, the first stage of the French system consists of three redundant wetlands. Only one of them is loaded; the others are not loaded but regenerated [37,38,58]. Thus, the mean load of the total required area results in 100 g COD/(m^2 d). Feeding breaks allow wetlands to regenerate. This can be used for the regeneration of seasonally high-loaded wetlands [27] or, as with the French system, by operating multiple stages in parallel and in series [58].

4.4. Comparability between Artificial and Real Wastewater

The treatment of the artificial DMAc wastewater results in comparable removal rates to treating the real wastewater (Figure 8a,b). Hence, the results of the artificial wastewater are basically generalizable. However, it can also be clearly seen that the TOC effluent concentrations of the artificial wastewater are lower than those of the real wastewater (Figure 10). Obviously, other substances contained in real wastewater, such as PVP and PSU, form low-degradable substances, which increase the concentration levels. The nitrogen content is based on DMAc, DMA, and PVP. Since nitrification was complete and the effluent contained no organically bound nitrogen, PVP must have been removed. Therefore, PSU is the possible reason for the higher effluent concentrations.

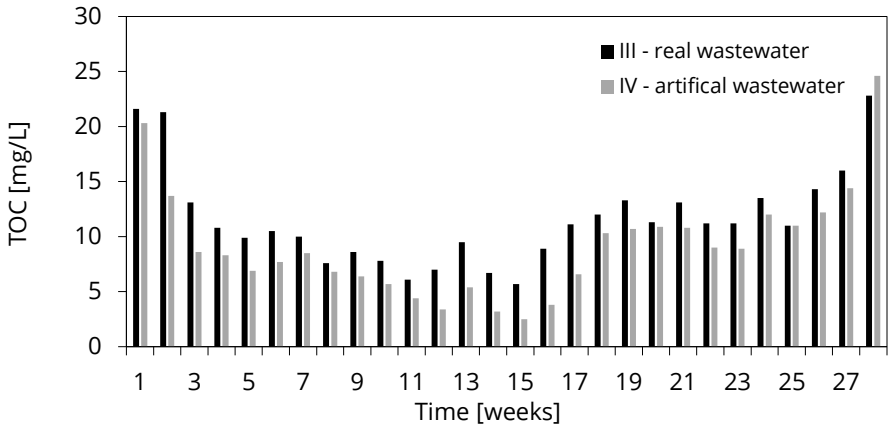

Figure 10. TOC effluent concentrations during the second test series when treating artificial and real wastewater.

4.5. Impact of the Inflow Concentration on the Effluent Concentration

As the DMAc influent concentrations increased, the TOC concentrations in the effluent also increased (Figure 11a–d). The total removal rate was not affected. Increasing the TOC inflow concentration from 0.78 g/L to 3.0 g/L resulted in an increase in the effluent TOC concentration of approximately 50% (Figure 11a–d), i.e., from 8.8 ± 1.2 mg/L to 13.2 ± 1.2 mg/L (test plant III, Figure 11c). As previously mentioned, the effluent concentrations of test plant III were higher than that of test plant IV (Figure 11a–d). However, the further increase of the TOC inflow concentration to 4.4 g/L moderately increased the effluent concentration of column IIIB to a mean value of 17.8 ± 7.1 mg/L. In contrast, the increase was significantly higher in test plant IV. Regardless, nitrification was complete in both test plants. However, the removal rates decreased clearly in the first stages. In parallel, the denitrification rate increased in both test plants (Figure 11e,f). Since the influent load was in the lower range of the first test series, overloading can be excluded.

Obviously, hydraulic conditions are the key factor for the declining removal rates. The hydraulic load gradually decreased from 80 L/(m^2 d) to 11 L/(m^2 d) with increasing concentrations. In the latter weeks, the specific hydraulic loading rate was only 2.7 L/(m^2 d). This is significantly less than the recommended value. For an equal water distribution at the filter surface, the specific hydraulic loading rate should reach 20 L/m^2 [37,38]. Due to the low hydraulic load, the water and, thus, the TOC load is unevenly distributed on the filter. Thus, several parts of the filter are not loaded, while the influent-fed part of the filter is overloaded. Consequently, the rapidly increasing effluent concentrations are due to uneven wastewater distribution on the filter. The increasing denitrification rate indicates a shortage of oxygen in layers that were aerobic before the increase in the inflow concentrations and the decrease in hydraulic load. Thus, the rapidly increasing effluent concentrations are due to the uneven distribution of wastewater on the filter. Although both test plants are designed and loaded similarly, the differences observed at high concentrations indicate an uneven wastewater distribution on the filters.

4.6. Effects of Seeding on the Start-Up Phase

Without seeding, the TOC removal rate reached 90% within three weeks. DMAc and DMA concentrations decreased below the limit of quantification in the same period. The removal efficiency stabilized at more than 96% after six weeks. The gradually increasing NH_4-N effluent concentrations observed during start-up are due to the hydrolysis of the nitrogen bound in DMAc. The more DMAc or DMA is degraded, the more NH_4-N is released. Nitrification starts after one month. The temporary nitrite accumulation also takes one month. Thus, nitrification is completely developed after two months. The mixing of fresh and seeded material significantly shortens the start-up phase. Thus, the TOC removal rate reached 97% after only one week. The start-up time for nitrification

is also shortened. After the third week, NH_4-N concentrations were below the limit of quantification. Nitrite accumulation was largely absent. At a load of 160 g COD/(m^2 d), the first stage should be fed four times a day. Fewer feed cycles result in the overloading of the first stage (see Section 3.3).

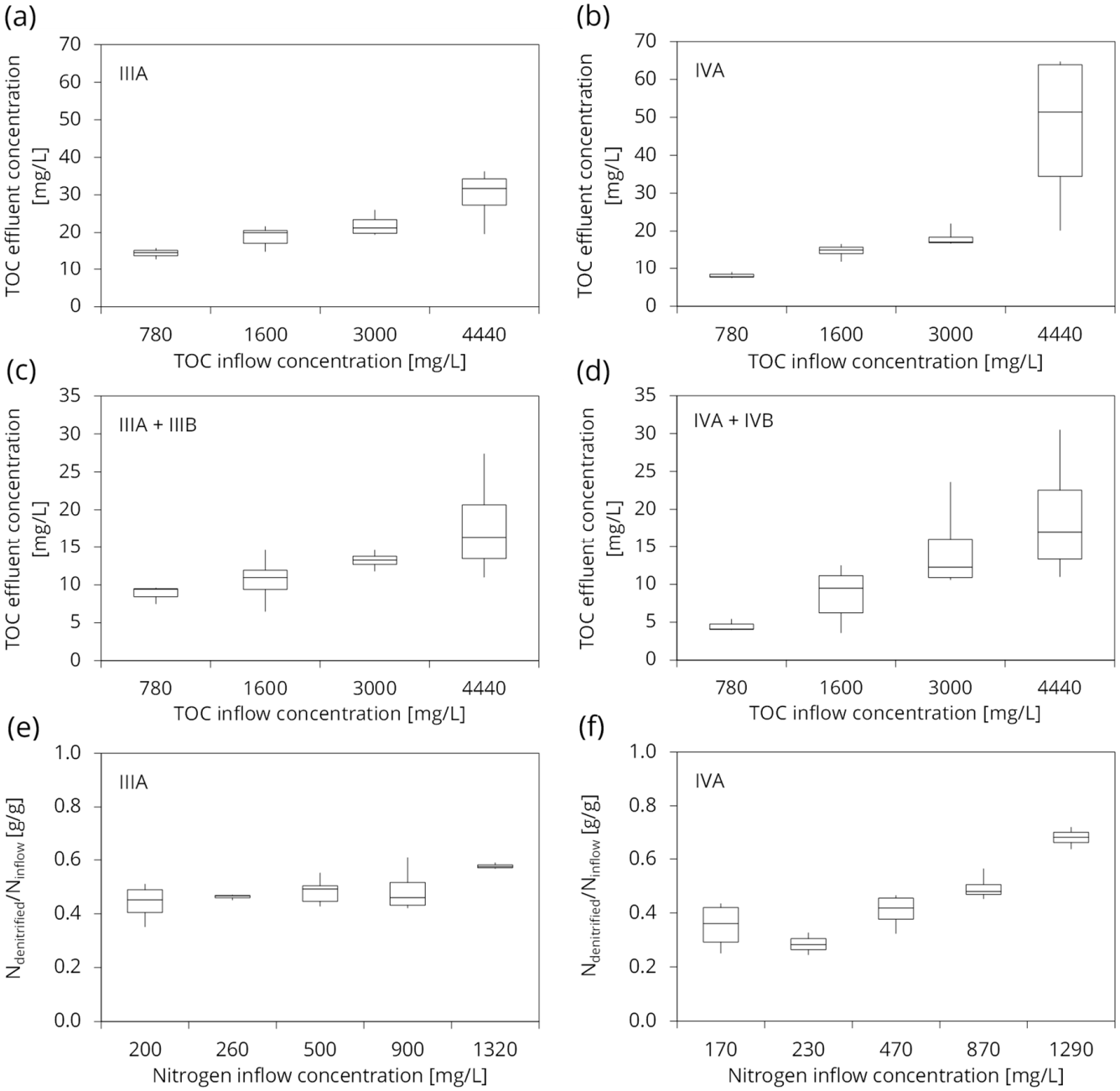

Figure 11. Impact of the inflow concentration on the effluent concentration during the second test series ((**a**,**b**): first stages; (**c**,**d**): second stages; (**e**,**f**): denitrification rate).

4.7. Assessment of the Removal Rates

The feed concentrations ranged between 1.1 and 8.0 g DMAc/L and 2.0 and 14.7 g COD/L. This is equal to the wastewater concentrations measured in a membrane manufacturing plant. Operational data of lab-scale and pilot-scale test plants described in the literature are comparable (see Table 4).

Table 4. Removal rates in comparison.

Source	Process	Parameter	Unit	DMAc	COD	TOC	TN	NH_4-N
[12]	Electrolysis + Hydro-lysis + SBR + MBR	Feed Conc. Removal	[mg/L] [%]	– –	4100 98	– –	150 57 [2]	15 –
[13] [1]	Upstream denitrification + MBR	Feed Conc. Removal	[mg/L] [%]	500–1700 100	1500–3000 93–96	450–1000 77–96	200–650 –	– –
[14]	Electrolysis + SBBR	Feed Conc. Removal	[mg/L] [%]	25–165 98	580–810 78	180–420 58	160–350 58	70–350 –
[15]	SBR	Feed Conc. Removal	[mg/L] [%]	51–77 –	519–702 –	– –	– –	88–105 –
[16]	Bioelectrical anaerobic system	Feed Conc. Removal	[mg/L] [%]	– –	1300–1700 19–31	– –	– –	30 –
This study	Two-stage VF wetland	Feed Conc. Removal [3]	[mg/L] [%]	877–7905 100	1461–14,321 >99	600–4442 >99	201–1318 58	– –

Notes: [1] Without data from oxygen-limited phases. [2] Calculated. [3] Without start-up phase. MBR . . . Membrane bioreactor. SBR . . . Sequencing batch reactor. SBBR . . . Sequencing batch biofilm reactor.

Regardless of the high load, the TOC removal efficiency was over 99%, which is higher than the biological treatment systems described in the literature (Table 4). At concentrations of 1.7 g DMAc/L and 4.1 g COD/L, 96% of COD and TOC [13] and 98% of COD [12] were removed (Table 4). Lower removal efficiencies were published by [14], who studied a combination of micro electrolysis and SBR. The difference between the COD removal efficiency (78%) and TOC (58%) is remarkable. Lower removal rates were also achieved when reactors were operated under oxygen shortage (see: [13]) or anaerobic conditions (see: [16]). In the named studies, complete nitrification was not achieved. In [15], the studied parameters affecting nitrification when treating wastewater containing DMAc, TOC, or DMAc removal rates are not published. However, it is obvious that in a nitrifying system, organic substances have largely been degraded. A comparison shows that very high removal rates, complete nitrification, and partial denitrification can be achieved with simple technologies such as VF wetlands, although the loading was significantly higher than those of municipal VF wetlands. The advantages of the studied VF wetlands compared to the biological treatment processes mentioned in Table 4 are higher TOC removal efficiencies and complete nitrification. In parallel, more than 40% of nitrogen was denitrified. Since VF wetlands are not artificially aerated, the energy requirement is lower compared to aerated sludge processes. The higher area required is unfavorable. However, the highly loaded first stage reduced the area requirement. The area of both stages was 75% less than the area of unaerated single-stage VF wetlands and 50% less than the area of two-stage VF wetlands designed according to the German standard DWA-A 262 [37,38]. A high organic and low hydraulic load can cause operational problems due to irregular distribution (Section 4.11). To avoid these problems, the effluent has to be recirculated.

4.8. Degradation Pathways and Microbial Composition

DMAc can be degraded by several microorganisms, e.g., *Rhodococcus* sp. *strain B83* [9], *Rhodococcus ruber HJM-8* [11], and *Paracoccus communis YBH-19 X* [11], via the intermediate methylacetmide and acetamide to acetate and ammonia. Not all of these bacteria are capable of using acetate as a substrate [9,11]. Therefore, acetate can initially accumulate and subsequently inhibit the degradation process [9,11]. When bacteria can utilize acetate, i.e., *Paracoccus communis YBH-19 X*, permanent accumulation does not occur [11]. Therefore, the efficiency in mixed cultures can be higher than in pure cultures since substances inhibiting one bacterial strain, e.g., acetate, can be degraded by another strain [11]. For the biodegradation of DMAc, this was proven by the combination of *Rhodococcus ruber HJM-8* and *Paracoccus communis YBH-19 X* [11]. Another possible pathway is degradation via the intermediate dimethylamine to acetate and ammonia [13]. In the present study, DMA was detectable over long periods of time. Thus, it is obvious that degradation occurs, as suggested by [13]. DMA was detected during the start-up phase and during oxygen shortage due to overloading. Strong DMA accumulation occurred at the beginning of the

start-up phase. Dependent on the operating conditions, DMA is largely or completely degraded. If DMA is not detected, this is not evidence that it is not formed. Biomass adaption to DMAc and DMA results in faster degradation [8], so DMAc and DMA are not detectable after all. However, if operating conditions deteriorate, DMA concentration may increase again.

Further support for the pathways discussed above can be gained from the microbiological analysis of 100 bacterial isolates per sample at three different stages in both artificial as well as real wastewater. The cultivable fraction of the DMAc degrading communities consisted of five main bacterial strains (Figure 12): *Aeromonas salmonicida*, *Brevibacillus non-reactive* (Reference genome: GCA_900637055.1), *Brucella anthropi* (GCA_012103185.1), *Chryseobacterium lacus* (GCA_003336205.1), and *Microbacterium oxydans* (GCA_003991855.1).

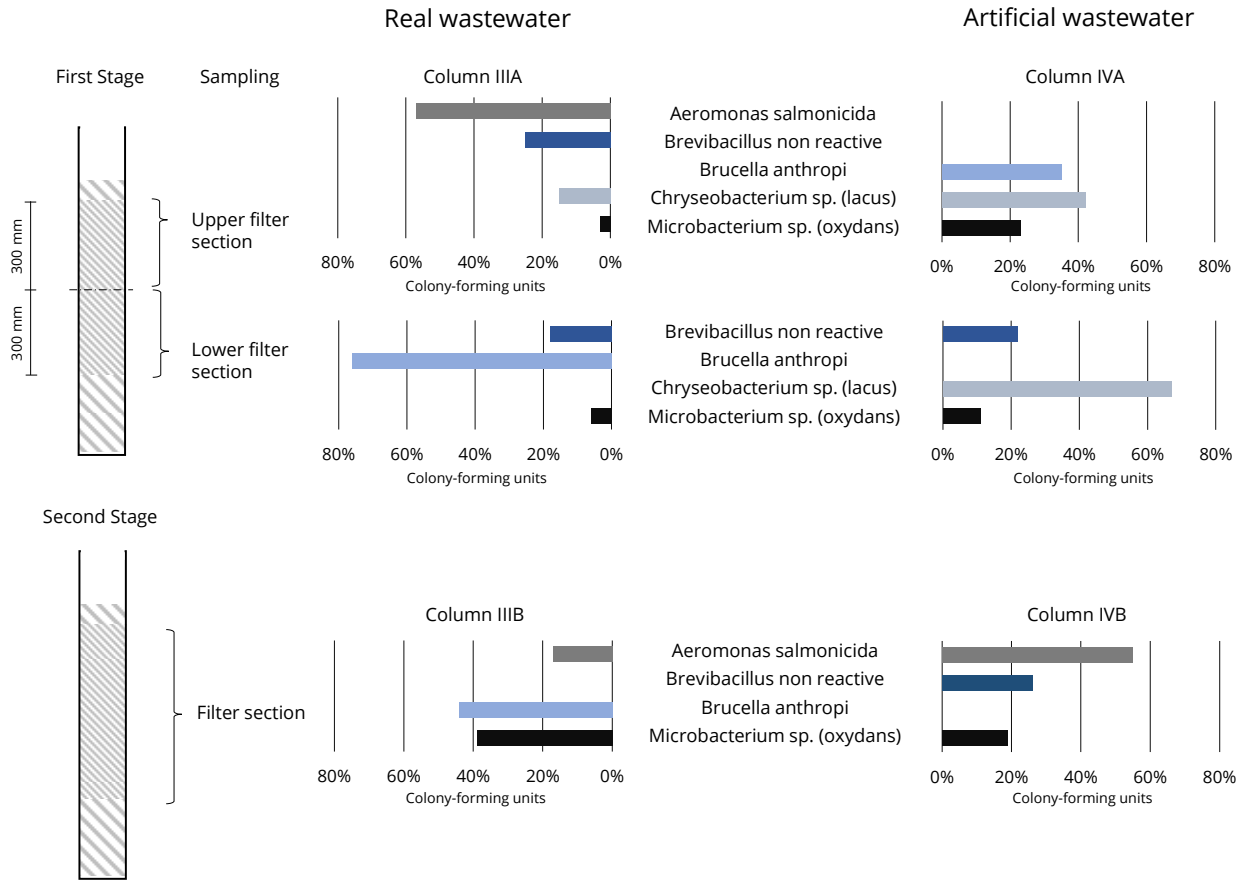

Figure 12. Microbial composition of the DMAc degrading communities.

Among these, *Brucella anthropi* was previously found to be able to utilize DMAc as the single carbon and nitrogen source [59]. It is further able to completely mineralize the sister compound DMF with high efficiency through a pathway highly similar to the here detected DMAc mineralization including DMA as an intermediate [59,60]. This involves the initial cleavage of DMF into the intermediates DMA and formates through a DMFase and the subsequent metabolism of the DMA into the second intermediate methylamine and further into formaldehyde and ammonia by means of two enzymes, dimethylamine dehydrogenase (EC 1.5.8.1) and methylamine dehydrogenase (EC 1.4.9.1). Genes encoding for the dimethylamine dehydrogenase were found in the *B. anthropi* reference genomes (KEGG: Oant_3262), while the methylamine dehydrogenase activity of *B. anthropi* had been experimentally verified by [59]. In addition to the detected enzymes and those described in the literature, an enzyme with trimethylamine-oxide aldolase activity was recognized. The detected enzyme shared a 97% coverage and 49% identity with an aminomethyltransferase enzyme in *E. coli* (AN: MRF39885.1). A docking

approach using the crystallographic structure of the *E. coli* enzyme as a receptor and DMAC as substrate showed that the latter could be stabilized in the active site with a $\Delta G_{binding} = -3$ Kcal mol^{-1} and a RMSD of 1.5 Å. While these parameters are not optimal, they suggest that the binding of the substrate could indeed take place. Overall, this could provide candidate enzymes for the initial DMAc cleavage into DMA and acetate, hence providing a complete degradation pathway in a single strain. In addition, *B. anthropi* was found to encode an homologous to Cytochrome P4502E1, previously reported to be involved in the catalysis of the second DMAc oxidation pathway via the intermediates methylacetamide and acetamide to acetate and ammonia [9,11], hence providing a second full degradation pathway in this species. Similarly, *Chryseobacterium lacus* was identified as a common member of DMF degrading communities [8,61], and while within its reference genome, not a complete DMAc breakdown pathway was found, genes coding for enzymes with dimethylamine dehydrogenase and trimethyl oxide aldolase activity were detected. The latter was also true for the remaining species.

Further, the potential accumulation of acetate, which as an inhibitor to complete DMAc degradation explains lower degradation speed in certain cultures of pure bacterial strains [9,11] and can be utilized by all five cultivated strains of the degradation consortium based on analysis of the reference genomes through a myriad of different enzymes (e.g., via acetate kinase (EC 2.7.2.1), acetyl-CoA synthase (EC 6.2.1.1), succinyl-Coa:acetate CoA-transferase (EC 2.8.3.18) or acetaldehyde dehydrogenase (EC 1.2.1.10)), providing that acetate-based inhibition should not appear.

Consequently, the pathways suggested based on chemical analysis underlying the complete degradation of DMAc in the consortium are supported by the different enzymes detected in silico for the isolates. Different bacterial species may contribute to environmental DMAc degradation, meaning that this process is multifactorial. Among the recovered species, *B. anthropi* might play a particularly important role. In spite of this, the substrate specificity of the recognized enzymes should be explored in future experiments. In addition, the high speed of DMAc degradation can be explained by an absence of acetate-based inhibition.

4.9. Evaluation of the COD Analyses

The digestion of the organic substances with dichromate during COD analysis according to the standard methods can be affected by the substances to be analyzed [62,63]. Not all of them are completely oxidizable, so the analyzed value can be either lower than the theoretical value or higher due to reactions between the oxidizing agent and certain ions of the substance to be analyzed [62–65]. An overview of the analyzed COD and theoretical oxygen demand (ThOD) of 582 substances is given by [63].

The ThOD of DMA is 2.13 g/g. Compared to the ThOD, DMA has a very low COD. According to data published in the literature, the COD is only 0.053 g/g [63] or 1.9% of the ThOD [62], i.e., 0.04 g/g. Tests with DMA standard solution (40%) have confirmed these values at 0.05 g/g. The ThOD of DMA is calculated according to Equation (8), and that of DMAc, according to Equation (9):

$$C_2H_7N + 3O_2 \rightarrow NH_3 + 2CO_2 + 2H_2O \quad (8)$$

$$C_4H_9NO + 5O_2 \rightarrow NH_3 + 4CO_2 + 3H_2O \quad (9)$$

The ThOD of DMAc is 1.86 g/g, and the analyzable COD is 1.6 g/g. Neglecting degradation byproducts and other wastewater components, the ThOD of wastewater containing mainly DMAc and DMA can be calculated according to Equation (10). The analyzable COD results from the COD analyses of DMAc and DMA according to Equation (11).

$$ThOD_{total} = 1.84 \text{ g ThOD/g DMAc} \cdot C_{DMAc} + 2.13 \text{ g ThOD/g DMA} \cdot C_{DMA} \quad (10)$$

ThOD is the theoretical oxygen demand [mg/L]; C_{DMAc} is the DMAc concentration [mg/L]; and C_{DMA} is the DMA concentration [mg/L].

$$COD = 1.58\ g\ COD/g\ DMAc \cdot C_{DMAc} + 0.05\ g\ COD/g\ DMA \cdot C_{DMA} \quad (11)$$

COD is the calculated, measurable COD [mg/L]; C_{DMAc} is the DMAc concentration [mg/L]; and C_{DMA} is the DMA concentration [mg/L].

During the tests, the measured COD effluent concentrations were significantly lower than the ThOD values. The correlation between the ThOD calculated according to Equation 10 and the measured COD concentrations gives a slope of 0.4 (Figure 13, $COD_{measured} = 0.38 \cdot ThOD + 34$). If the calculated COD according to Equation 11 is used instead of the ThOD, both the measured and the calculated COD largely agree (Figure 13, $COD_{measured} = 0.88 \cdot COD + 84$). The Offset is due to degradation products and biomass compounds.

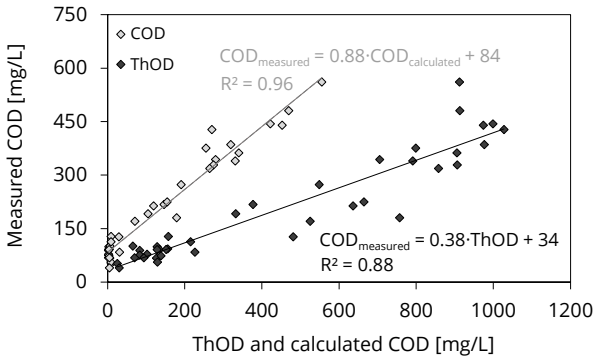

Figure 13. Comparison of the ThOD and COD values.

Hence, COD analyses are not suitable for the analysis of wastewater from the membrane industry, containing mainly DMAc and DMA, because the actual wastewater load is underestimated. On the other hand, this overestimates COD removal rates. Therefore, the TOC value is suggested to characterize wastewater containing DMAc and DMA. Based on the COD:TOC ratio, implausible COD concentrations can be identified. As long as DMAc is largely degraded to DMA only, the COD:TOC ratio is low and in the range of 1. When degradation is complete, it increases to about 2.9.

4.10. Ecotoxicological Effects

The applied in vitro bioassays are useful tools to detect (eco-)toxicological effects during the treatment processes of wastewater. These effect-based methods can also detect effects of unknown substances or products generated during treatment, as it was found in plant I where mutagenic effects were detected that were not found in the initial influent. On the other hand, effect-based methods are usually limited in identifying individual substances responsible for the effect. Therefore, it cannot be clarified which specific substances were responsible for the mutagenic effects observed in plant I during the experiment in the first weeks. Interestingly, mutagenic effects could be only detected with the strain TA100 in the applied Ames test, which identifies substances responsible for a base-pair substitution. One of the possible compounds responsible for the base-pair substitution could be nitrite [66] since it was measured in high concentrations during the first weeks of the run in plant I. Nitrite was identified to produce base-pair substitution but did not lead to frameshift mutations which could be detected by strain TA98 [66]. In the wastewater of the present study, moderate or high mutagenic effects could be detected for base-pair substitution but not for frameshift mutation. This correlated mostly with high concentrations of nitrite measured in these samples. Whether other substances also lead to an increase in such mutations cannot be ruled out. Genotoxicity measured using the in vitro micronucleus test is a well-established international approach for testing wastewater [67]

and effluent toxicity (reviewed by [68]). Further, many substances were found to be genotoxic in MNvit tests [69]. The DCFH assay to identify ROS formations is described as not highly specific but can detect different types of ROS produced and is widely used as a qualitative marker of cellular oxidative stress [48,70]. Finally, DMAc could lead to moderate genotoxicity in the MNvit test and high-level formation of ROS (DCFH assay) since these effects were identified for the initial influent containing 1125 mg/L DMAc. Further, this influent concentration of DMAc did not lead to mutagenic effects (base-pair substitution, frameshift mutation).

4.11. Recommendations

Basically, the researched two-stage VF wetland is capable of removing DMAc. Temporary high loads of more than 300 g COD/(m^2 d) are treatable without impairing the removal rate. Based on the results, 160 g COD/(m^2 d) seems to be a realistic value for the design load of the first stage. However, further research on a larger scale is needed for a reliable evaluation.

No external nitrogen source is needed for DMAc degradation. Microorganisms can utilize the nitrogen bound in DMAc. The biomass nitrogen demand is 11.5% of the nitrogen supplied with DMAc. This equates to a COD:N ratio of 200:2, which is lower than the typical ratio of 200:5 [71,72]. The phosphorous demand is also lower than expected. The COD:P ratio is 200:0.3. Since [31] also found reduced nutrient demand when treating industrial wastewater in VF wetlands, this may be due to the reuse of released nutrients during biomass decay within the filter material.

Since nitrate supports the oxygen conditions in the first stage, nitrification should basically be targeted. Due to the high nitrogen content of DMAc, bicarbonate dosing is required. Although bicarbonate is released again during the degradation of DMAc, it is not sufficient to compensate for the demand for nitrification. Since denitrification recovers bicarbonate, the dosage may decrease as denitrification increases.

For better wastewater distribution on the filter surface at low hydraulic load, effluent recirculation into the inflow is useful. Assuming a feed TOC concentration of 4.4 g/L, a hydraulic load of 11 L/(m^2 d), a recirculation ratio of two ($Q_{recirculation}/Q_{inflow}$), and four feeding cycles per day, the specific hydraulic loading rate increases from 2.7 L/m^2 to 8.2 L/m^2 per dose. To ensure a specific hydraulic loading rate of 20 L/m^2, the recirculation ratio increases to six. Since the number of feeding cycles affects the oxygen conditions at high loading in the first stage, it is not recommended to reduce the number of feeding cycles to increase the specific hydraulic loading rate.

5. Conclusions

Highly loaded two-stage VF wetlands are a simple and low-energy technology for treating DMAC-containing wastewater. The TOC removal efficiency is higher than the results published in the literature. Additionally, the nitrogen is completely nitrified. DMAc is degraded via the intermediate DMA by different bacteria.

The COD value is not suitable for the analysis of wastewater containing DMAc and DMA. Therefore, the TOC value should be used for monitoring wastewater treatment.

Since a substantial part of the degradation process occurs in the first stage, proper material selection is an important factor in ensuring proper oxygen conditions. Seeding of the filter material is not needed, but it shortens the start-up period, and it may prevent high nitrite accumulation. Without seeding, nitrite accumulation can take several weeks and reach very high concentrations of up to 140 mg NO_2-N/L.

DMAc removal in VF wetlands seems to be a promising approach. However, further research is needed. This should focus on the long-time operation of the wetland, especially whether collimation processes occur in the first stage and how these affect the removal rate. Furthermore, the effect of load changes on the nitrification rate and the oxygen conditions needs to be investigated.

Author Contributions: Conceptualization, T.S., A.R., S.S.; methodology, T.S., S.S., A.R., D.F.-S., A.S.; validation, T.S., S.S., A.R., D.F.-S.; formal analysis, T.S., A.R., S.S., A.X.E., A.S.; investigation, C.K., T.S., A.R., S.S., A.S., D.F.-S.; data curation, T.S., C.K., S.S., A.R.; writing—original draft preparation, T.S., S.S., A.X.E.; visualization, T.S., S.S.; supervision, P.K.; project administration, T.S.; funding acquisition, A.R., T.S., S.S., D.F.-S. All authors have read and agreed to the published version of the manuscript.

Funding: This research was funded by the German Federal Ministry of Education and Research, grant number: 02WV1566. The Article Processing Charge (APC) was funded by the German Federal Ministry of Education and Research.

Data Availability Statement: The data presented in this study are available in article.

Acknowledgments: The authors are thankful for the special technical support of Markus Ahnert, Heike Brückner, Sinaida Heidt, and Ulrike Gebauer from the Institute of Urban and Industrial Water Management, Juliane Isler and Claudia Seifert (both from the Institute of Hydrobiology), Marie Schnelle, Max Bachofner, Till Teichert, and Philipp Wockatz from the B. Braun Avitum Saxonia GmbH, Yvonne Kaschel, Claudia Spittang, and Sven Zschunke from the CUP Laboratorien Dr. Freitag GmbH, and for language revision by Uli Klümper (Institute of Hydrobiology). Further, the authors would like to thank the research assistants of the Institute of Urban and Industrial Water Management, Sophie Hoyer, Caroline Breitenberger, Roman Ledwa, Tobias Wanka, Peter Trautmann, and Moritz Bayer for their support in operating the test plants.

Conflicts of Interest: The authors declare no conflict of interest.

Appendix A. Tables

Table A1. Load (L), removal rates (η), feed and effluent concentrations (C) during the first test series (1st row: mean ± standard deviation, 2nd row: min–max).

Parameter	Unit	First Stage		Combination			
		IA	IIA	IA + IB	IA + IC	IIA + IIB	IIA + IIC
$L_{A,TOC}$	[g/(m^2 d)]	61 ± 15 47–92	63 ± 16 51–97	61 ± 15 47–92	61 ± 15 47–92	63 ± 16 51–97	63 ± 16 51–97
η_{TOC}	[%]	81 ± 20 0–94	88 ± 16 28–98	94 ± 11 46–99	90 ± 18 25–99	94 ± 11 47–99	93 ± 13 38–99
$C_{TOC,feed}$	[mg/L]	768 ± 197 621–1164	768 ± 197 621–1164	768 ± 197 621–1164	768 ± 197 621–1164	768 ± 197 621–1164	768 ± 197 621–1164
$C_{TOC,eff}$	[mg/L]	129 ± 118 54–623	77 ± 94 23–450	34 ± 65 6.5–319	56 ± 97 12–443	37 ± 71 9.2–350	44 ± 76 13–374
$L_{A,DMAc}$	[g/(m^2 d)]	111 ± 28 85–166	115 ± 29 93–176	111 ± 28 85–166	111 ± 28 85–166	115 ± 29 93–176	115 ± 29 93–176
η_{DMAc}	[%]	93 ± 20 10–100	95 ± 14 37–100	98 ± 8.1 61–100	97 ± 11 47–100	98 ± 8.4 60–100	98 ± 9.3 56–100
$C_{DMAc,feed}$	[mg/L]	1391 ± 357 1125–2109	1391 ± 357 1125–2109	1391 ± 357 1125–2109	1391 ± 357 1125–2109	1391 ± 357 1125–2109	1391 ± 357 1125–2109
$C_{DMAc,eff}$	[mg/L]	71 ± 217 0.1–1017	50 ± 151 0.1–714	18 ± 87 0.1–415	25 ± 119 0.1–568	21 ± 101 0.1–484	22 ± 100 0.1–482
$C_{DMA,eff}$	[mg/L]	98 ± 62 25–255	53 ± 69 5.0–285	22 ± 58 5.0–235	44 ± 110 5.0–383	20 ± 51 5.0–222	22 ± 50 5.0–211
$L_{A,TKN}$	[g/(m^2 d)]	18 ± 4.5 14–27	18 ± 4.6 15–28	18 ± 4.5 14–27	18 ± 4.5 14–27	18 ± 4.6 15–28	18 ± 4.6 15–28
η_{TKN}	[% TKN_{feed}]	38 ± 25 5.5–72	69 ± 34 7.8–97	73 ± 36 10–99	61 ± 39 2–98	78 ± 32 21–99	76 ± 34 20–99
$\eta_{nitrification}$	[% TKN_{feed}]	31 ± 23 0.6–61	62 ± 32 4.6–87	66 ± 35 1.2–89	54 ± 37 1.1–87	69 ± 30 10–87	67 ± 32 9.7–88

Table A1. *Cont.*

Parameter	Unit	First Stage		Combination			
		IA	**IIA**	**IA + IB**	**IA + IC**	**IIA + IIB**	**IIA + IIC**
$\eta_{dentrification}$	[% TKN_{feed}]	31 ± 23 0.0–61	30 ± 18 4.1–58	29 ± 24 0.0–60	32 ± 23 0.0–63	32 ± 14 8.5–54	33 ± 16 9.2–59
$C_{TKN,feed}$	[mg/L]	224 ± 58 181–340	224 ± 58 181–340	224 ± 58 181–340	224 ± 58 181–340	224 ± 58 181–340	224 ± 58 181–340
$C_{TKN,eff}$	[mg/L]	123 ± 34 71–191	52 ± 60 6.2–167	41 ± 58 3.0–149	66 ± 68 4.4–152	38 ± 56 3.0–143	39 ± 59 3.0–143
$C_{NH4-N,eff}$	[mg/L]	80 ± 31 7.8–134	26 ± 35 3.0–108	30 ± 48 3.0–134	47 ± 59 3.0–151	26 ± 45 3.0–130	27 ± 45 3.0–126
$C_{NO3-N,eff}$	[mg/L]	1.1 ± 0.1 1.0–1.6	53 ± 46 1–103	56 ± 43 1.0–113	34 ± 38 1.0–89	69 ± 51 1.0–118	62 ± 52 1.0–118
$C_{NO2-N,eff}$	[mg/L]	0.6 ± 1.7 0.0–8.0	19 ± 33 0.0–102	22 ± 45 0.0–142	18 ± 29 0.0–88	14 ± 36 0.0–132	19 ± 39 0.0–128

Table A2. Load (L), removal rates (η), feed and effluent concentrations (C) during the second test series (first row: mean ± standard deviation, second row: min–max).

Parameter	Unit	First Stage		Combination	
		IIIA	**IVA**	**IIIA + IIIB**	**IVA + IVB**
$L_{A,TOC}$	[g/(m^2 d)]	47 ± 2.1 42–49	47 ± 2.1 44–52	47 ± 2.1 42–49	47 ± 2.1 44–52
η_{TOC}	[%]	90 ± 12 64–99	91 ± 14 58–99	99 ± 1.0 96–100	99 ± 0.6 98–100
$C_{TOC,feed}$	[g/L]	1.7 ± 1.4 0.6–4.4	1.7 ± 1.4 0.6–4.4	1.7 ± 1.4 0.6–4.4	1.7 ± 1.4 0.6–4.4
$C_{TOC,eff}$	[mg/L]	64 ± 74 13–244	67 ± 75 15–249	13 ± 4.7 6.5–27	11 ± 6.3 3.6–31
$L_{A,DMAc}$	[g/(m^2 d)]	76 ± 6.3 69–87	86 ± 3.8 81–95	76 ± 6.3 69–87	86 ± 3.8 81–95
η_{DMAc}	[%]	96 ± 7.2 79–100	95 ± 9.8 68–100	100 ± 0.0 100	100 ± 0.0 100
$C_{DMAc.feed}$	[g/L]	2.9 ± 2.6 0.9–7.9	3.1 ± 2.5 1.1–8.0	2.9 ± 2.6 0.9–7.9	3.1 ± 2.5 1.1–8.0
$C_{DMAc,eff}$	[mg/L]	37 ± 64 0.1–190	54 ± 107 0.1–343	0.1 ± 0.0 0.1	0.1 ± 0.0 0.1
$C_{DMA,eff}$	[mg/L]	125 ± 130 5.0–346	91 ± 102 5.0–248	5.0 ± 0.0 5.0–5.0	5.0 ± 0.7 5.0–8.0
$L_{A,TKN}$	[g/(m^2 d)]	15 ± 1.1 13–16	14 ± 0.6 13–15	15 ± 1.1 13–16	14 ± 0.6 13–15
η_{TKN}	[% TKN_{feed}]	83 ± 23 0–100	82 ± 26 0–99	95 ± 12 49–100	96 ± 7.8 62–100
$\eta_{nitrification}$	[% TKN_{feed}	79 ± 16 36–89	77 ± 17 34–88	85 ± 12 39–89	85 ± 7.7 51–88
$\eta_{dentrification}$	[% TKN_{feed}]	46 ± 11 9.4–61	42 ± 14 18–72	46 ± 10 20–62	43 ± 14 25–72
$C_{TKN,feed}$	[mg/L]	532 ± 406 201–1318	502 ± 407 175–1294	532 ± 406 201–1318	502 ± 407 175–1294

Table A2. *Cont.*

Parameter	Unit	First Stage		Combination	
		IIIA	IVA	IIIA + IIIB	IVA + IVB
$C_{TKN,eff}$	[mg/L]	33 ± 44 3.0–146	35 ± 39 3.9–131	11 ± 23 3.2–103	9.5 ± 16 3.1–68
$C_{NH4\text{-}N,eff}$	[mg/L]	9.5 ± 13 3.0–58	14 ± 16 3.0–60	9.3 ± 23 3.0–102	7.3 ± 16 3.0–68
$C_{NO3\text{-}N,eff}$	[mg/L]	173 ± 152 1.0–420	146 ± 119 1.0–373	197 ± 140 1.0–455	182 ± 107 3.0–386
$C_{NO2\text{-}N,eff}$	[mg/L]	0.5 ± 0.9 0–2.8	5.8 ± 9.4 0–36	0.2 ± 0.3 0–1.4	0.2 ± 0.5 0–2.7

Appendix B. Figures

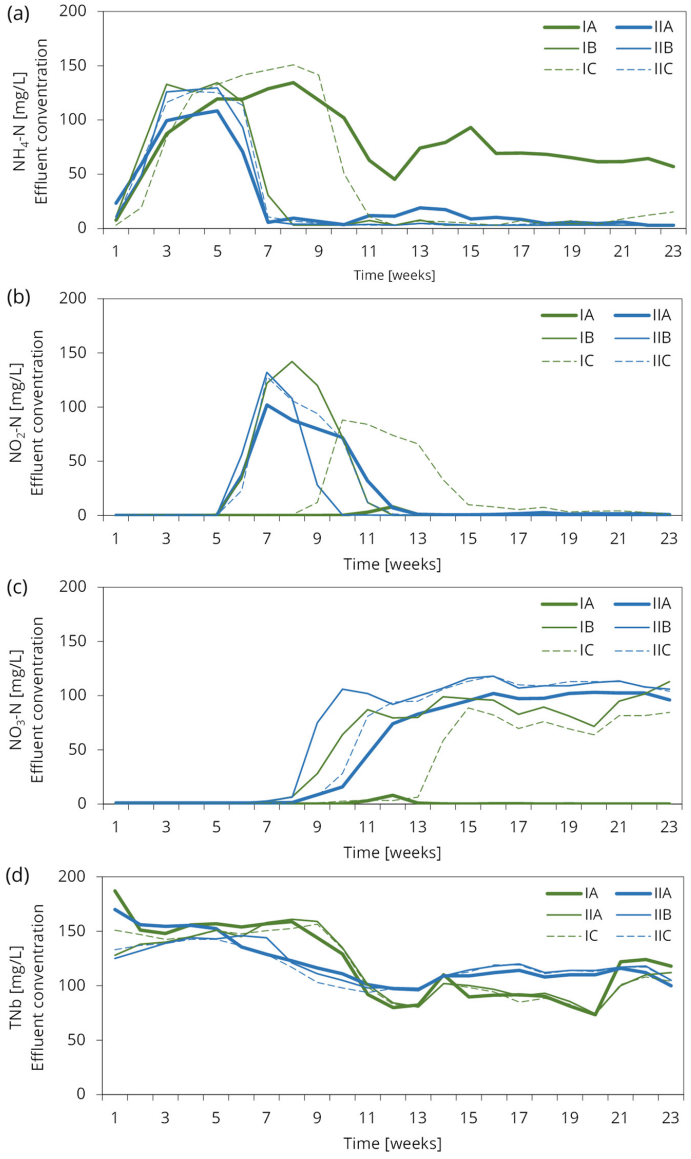

Figure A1. Effluent concentrations of the parameters NH_4-N (**a**), NO_2-N (**b**), NO_3-N (**c**) TNb (**d**) during the first test series.

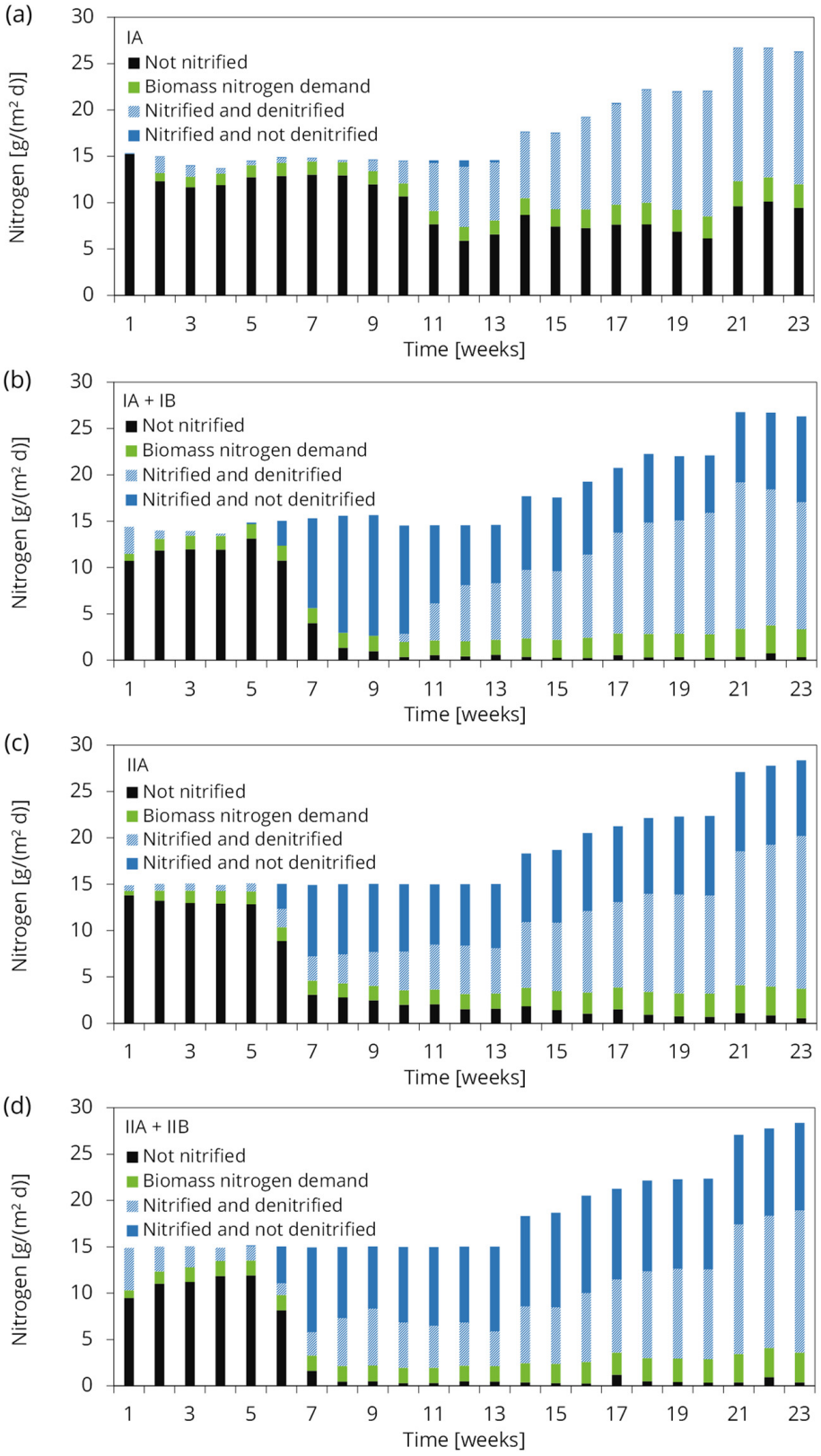

Figure A2. Nitrogen balance during the first test series ((**a**): first stage of the 1st test plant, (**b**): overall balance for IA + IB, (**c**): first stage of the 2nd test plant, (**d**): overall balance for IIA + IIB).

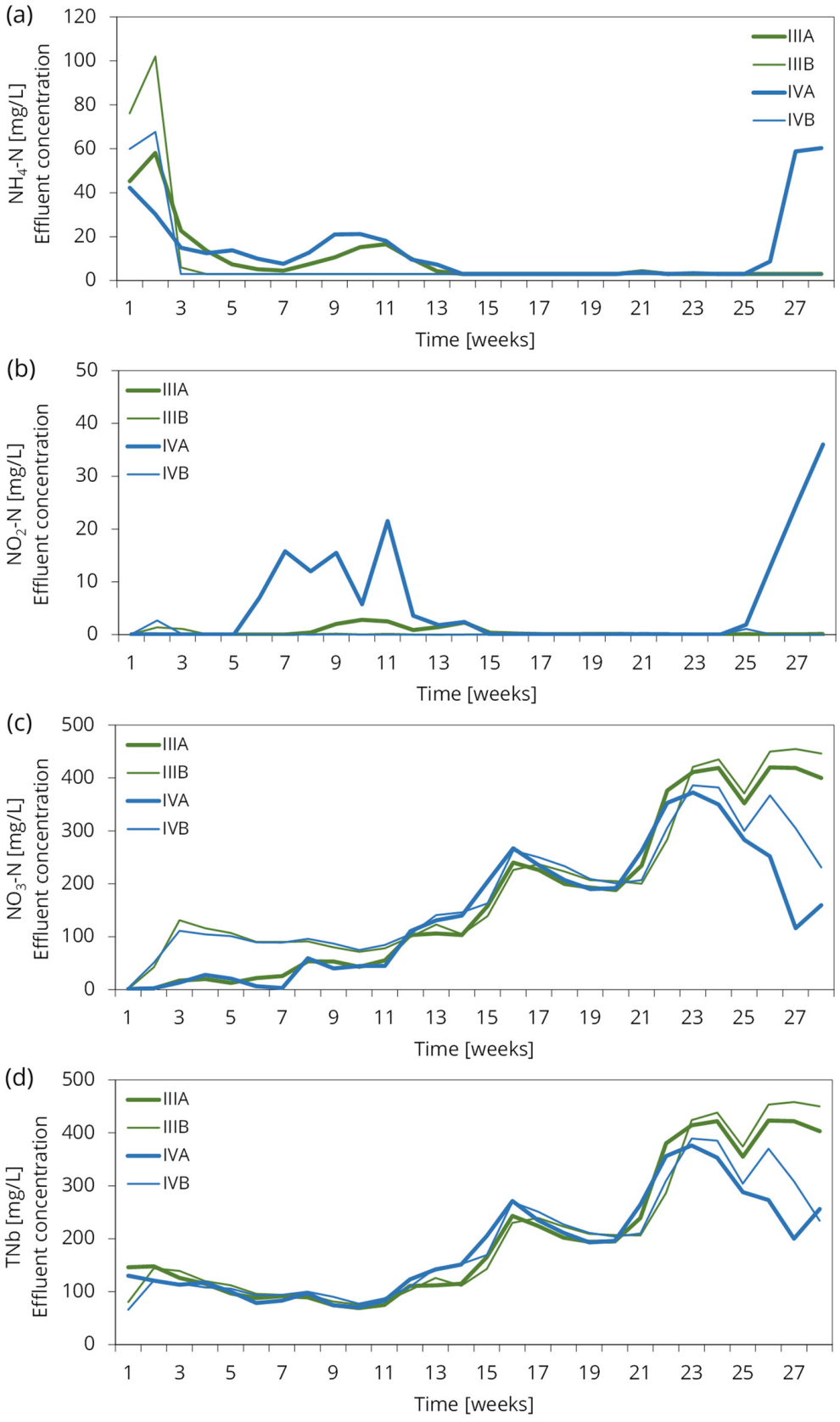

Figure A3. Effluent concentrations of the parameters NH_4-N (**a**), NO_2-N (**b**), NO_3-N (**c**) TNb (**d**) during the second test series.

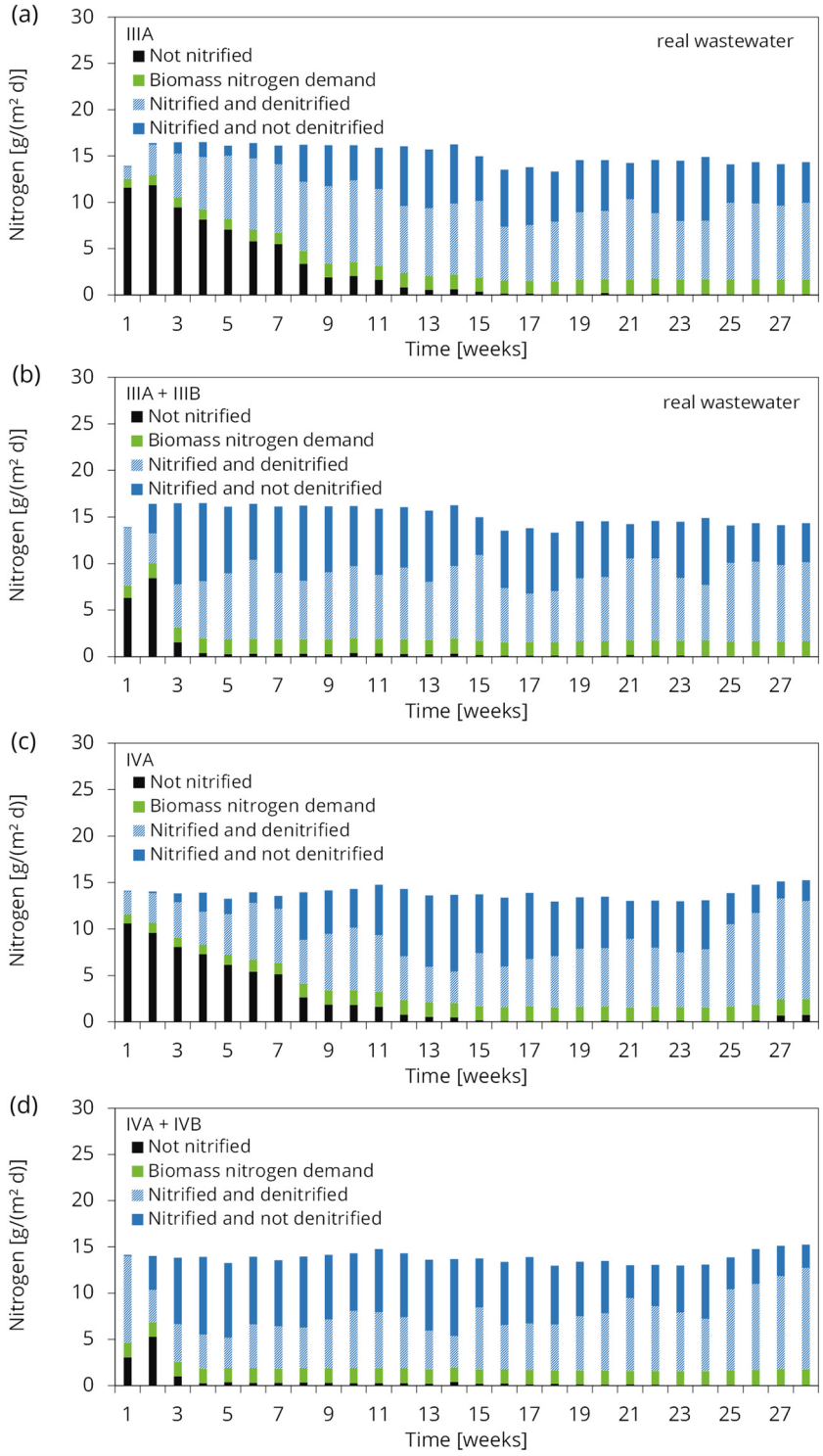

Figure A4. Nitrogen balance during the second test series ((**a**): first stage of the 3rd test plant, (**b**): overall balance for IIIA + IIIB, (**c**): first stage of the 4th test plant, (**d**): overall balance for IVA + IVB).

References

1. Dong, X.; Lu, D.; Harris, T.A.L.; Escobar, I.C. Polymers and Solvents Used in Membrane Fabrication: A Review Focusing on Sustainable Membrane Development. *Membranes* **2021**, *11*, 309. [CrossRef] [PubMed]
2. Figoli, A.; Marino, T.; Simone, S.; Di Nicolò, E.; Li, X.-M.; He, T.; Tornaghi, S.; Drioli, E. Towards Non-Toxic Solvents for Membrane Preparation: A Review. *Green Chem.* **2014**, *16*, 4034. [CrossRef]

3. Peinemann, K.P.; Nunes, S.P. Polymermembranen. In *Membranen: Grundlagen, Verfahren und Industrielle Anwendungen*; Ohlrogge, K., Ebert, K., Eds.; WILEY-VCH Verlag GmbH & Co. KGaA: Weinheim, Germany, 2006; pp. 1–22. ISBN 978-3-527-30979-5.
4. Zou, D.; Nunes, S.P.; Vankelecom, I.F.J.; Figoli, A.; Lee, Y.M. Recent Advances in Polymer Membranes Employing Non-Toxic Solvents and Materials. *Green Chem.* **2021**, *23*, 9815–9843. [CrossRef]
5. ECHA Annex XV Restriction Report. *Proposal for a Restriction. Substance Names(s): N,N-Dimethylacetamide (DMAC) and 1-Ethylpyrrolidin-2-One (NEP)*; European Chemicals Agency: Helsinki, Finland; Bureau REACH, National Institute for Public Health and the Environment (RIVM): Bilthoven, The Netherlands, 2022.
6. German Environment Agency (Umweltbundesamt—UBA). Bekanntmachung der bereits durch die oder auf Grund der Verwaltungsvorschrift wassergefährdende Stoffe eingestuften Stoffe, Stoffgruppen und Gemische gemäß § 66 Satz 1 der Verordnung über Anlagen zum Umgang mit wassergefährdenden Stoffen. *Bundesanzeiger*, 10 August 2017; p. B5.
7. Li, Y.; Wu, H.; Liang, X.; Rong, C.; Chen, H. Experimental Study of Waste Concentration by Mechanical Vapor Compression Technology. *Desalination* **2015**, *361*, 46–52. [CrossRef]
8. Bhojani, G.; Jani, S.; Saha, N.K. Facile biodegradation of N,N-dimethylformamide, N,N-dimethylacetamide and N-methyl-2-pyrrolidone by source-derived Bacillus strain APS1 for water reclamation and reuse. *J. Clean. Prod.* **2022**, *334*, 130098. [CrossRef]
9. Chen, X.; Yang, C.; Wang, W.; Ge, B.; Zhang, J.; Liu, Y.; Nan, Y. Biodegradation of N,N-Dimethylacetamide by Rhodococcus Sp. Strain B83 Isolated from the Rhizosphere of Pagoda Tree. *J. Environ. Sci.* **2017**, *53*, 88–98. [CrossRef]
10. Santoshkumar, M.; Veeranagouda, Y.; Lee, K.; Karegoudar, T.B. Utilization of Aliphatic Nitrile by Paracoccus Sp. SKG Isolated from Chemical Waste Samples. *Int. Biodeterior. Biodegrad.* **2011**, *65*, 153–159. [CrossRef]
11. Yuan, B.; Yao, J.; Wang, Z.; Dai, L.; Zhao, M.; Hrynsphan, D.; Tatsiana, S.; Chen, J. Increasing N,N-Dimethylacetamide Degradation and Mineralization Efficiency by Co-Culture of Rhodococcus Ruber HJM-8 and Paracoccus Communis YBH-X. *Chemosphere* **2022**, *303*, 134935. [CrossRef]
12. Guo, T.; Ji, Y.; Zhao, J.; Horn, H.; Li, J. Coupling of Fe-C and Aerobic Granular Sludge to Treat Refractory Wastewater from a Membrane Manufacturer in a Pilot-Scale System. *Water Res.* **2020**, *186*, 116331. [CrossRef]
13. Zhuo, M.; Abass, O.K.; Zhang, K. New Insights into the Treatment of Real N,N-Dimethylacetamide Contaminated Wastewater Using a Membrane Bioreactor and Its Membrane Fouling Implications. *RSC Adv.* **2018**, *8*, 12799–12807. [CrossRef] [PubMed]
14. Jie, L.; Yongfeng, S.; Yae, W.; Yuexi, Z.; Jinyuan, J. Treatment of Acrylic Fiber Wastewater Treatment Using Combined Process of Iron Carbon Micro-Electrolysis and SBBR. In Proceedings of the 2011 International Conference on Computer Distributed Control and Intelligent Environmental Monitoring, Changsha, China, 19–20 February 2011; pp. 2356–2359.
15. Li, J.; Yu, D.; Zhang, P. Partial Nitrification in a Sequencing Batch Reactor Treating Acrylic Fiber Wastewater. *Biodegradation* **2013**, *24*, 427–435. [CrossRef] [PubMed]
16. Xie, J.; Chang, Y.; Chen, C.; Ma, J.; Liu, H.; Cui, H.; Zhang, T.C. Bioelectrochemical Systems with a Cathode of Stainless-Steel Electrode for Treatment of Refractory Wastewater: Influence of Electrode Material on System Performance and Microbial Community. *Bioresour. Technol.* **2021**, *342*, 125959. [CrossRef] [PubMed]
17. Behrouzeh, M.; Abbasi, M.; Osfouri, S.; Dianat, M.J. Treatment of DMSO and DMAC Wastewaters of Various Industries by Employing Fenton Process: Process Performance and Kinetics Study. *J. Environ. Chem. Eng.* **2020**, *8*, 103597. [CrossRef]
18. Li, J.; Luan, Z.; Yu, L.; Ji, Z. Pretreatment of Acrylic Fiber Manufacturing Wastewater by the Fenton Process. *Desalination* **2012**, *284*, 62–65. [CrossRef]
19. Li, W.; Chen, M.; Zhong, Z.; Zhou, M.; Xing, W. Hydroxyl Radical Intensified Cu2O NPs/H2O2 Process in Ceramic Membrane Reactor for Degradation on DMAc Wastewater from Polymeric Membrane Manufacturer. *Front. Environ. Sci. Eng.* **2020**, *14*, 102. [CrossRef]
20. Yuan, Y.; Geng, F.; Shi, B.; Lai, B. Simultaneous Thermal Activation of Persulfate/Fenton System for High-Concentration N,N-Dimethylacetamide Degradation: Parameter Optimization and Degradation Mechanism. *Environ. Eng. Sci.* **2019**, *36*, 12–22. [CrossRef]
21. Zhou, M.; Li, W.; Chen, M.; Zhong, Z.; Xing, W. Synthesis of CuxCo3−xO4 Nanocatalyst for Degradation of Nitrogenous Organic Wastewater in Fenton-like Membrane Reactor. *Appl. Water Sci.* **2022**, *12*, 57. [CrossRef]
22. Xiong, Z.; Li, J.; Li, Y.; Yuan, Y.; Jiang, Y.; Yao, G.; Lai, B. Simultaneously Enhanced Degradation of N,N-Dimethylacetamide and Reduced Formation of Iron Sludge by an Efficient Electrolysis Catalyzed Ozone Process in the Presence of Dissolved Silicate. *J. Hazard. Mater.* **2021**, *406*, 124725. [CrossRef]
23. Cooper, P. A Review of the Design and Performance of Vertical-Flow and Hybrid Reed Bed Treatment Systems. *Water Sci. Technol.* **1999**, *40*, 1–9. [CrossRef]
24. von Felde, K.; Kunst, S. N- and COD-Removal in Vertical-Flow Systems. *Water Sci. Technol.* **1997**, *35*, 79–85. [CrossRef]
25. Vymazal, J. Removal of Nutrients in Various Types of Constructed Wetlands. *Sci. Total Environ.* **2007**, *380*, 48–65. [CrossRef] [PubMed]
26. Dotro, G.; Langergraber, G.; Molle, P.; Nivala, J.; Puigagut, J.; Stein, O.; von Sperling, M. *Treatment Wetlands*; Biological Wastewater Treatment Series; IWA Publishing: London, UK, 2017; Volume 7, ISBN 978-1-78040-877-4.
27. Schalk, T.; Marx, C.; Haupt, A.; Kühn, V.; Krebs, P. Long-Term Effects of Sulfide on Ammonia Oxidation and Nitrite Accumulation in a Seasonally Loaded Vertical Flow Constructed Wetland. *Wetlands* **2020**, *40*, 205–222. [CrossRef]
28. Cooper, P. Constructed Wetlands and Reed-Beds: Mature Technology for the Treatment of Wastewater from Small Populations. *Water Environ. J.* **2001**, *15*, 79–85. [CrossRef]

29. Martinez-Guerra, E.; Jiang, Y.; Lee, G.; Kokabian, B.; Fast, S.; Truax, D.D.; Martin, J.L.; Magbanua, B.S.; Gude, V.G. Wetlands for Wastewater Treatment. *Water Env. Res.* **2015**, *87*, 1095–1126. [CrossRef] [PubMed]
30. Masi, F.; Rochereau, J.; Troesch, S.; Ruiz, I.; Soto, M. Wineries Wastewater Treatment by Constructed Wetlands: A Review. *Water Sci. Technol.* **2015**, *71*, 1113–1127. [CrossRef]
31. Paing, J.; Serdobbel, V.; Welschbillig, M.; Calvez, M.; Gagnon, V.; Chazarenc, F. Treatment of High Organic Content Wastewater from Food-Processing Industry with the French Vertical Flow Constructed Wetland System. *Water Sci. Technol.* **2015**, *72*, 70–76. [CrossRef]
32. Pascual, A.; De la Varga, D.; Soto, M.; Van Oirschot, D.; Kilian, R.M.; Álvarez, J.A.; Carvalho, P.; Brix, H.; Arias, C.A. Aerated Constructed Wetlands for Treatment of Municipal and Food Industry Wastewater. In *Constructed Wetlands for Industrial Wastewater Treatment*; Alexandros, S., Ed.; Wiley: Hoboken, NJ, USA, 2018; ISBN 978-1-119-26834-5.
33. Haberl, R.; Grego, S.; Langergraber, G.; Kadlec, R.H.; Cicalini, A.-R.; Dias, S.M.; Novais, J.M.; Aubert, S.; Gerth, A.; Thomas, H.; et al. Constructed Wetlands for the Treatment of Organic Pollutants. *J. Soils Sediments* **2003**, *3*, 109–124. [CrossRef]
34. Al-Isawi, R.H.K.; Sani, A.; Almuktar, S.A.A.A.N.; Scholz, M. Vertical-Flow Constructed Wetlands Treating Domestic Wastewater Contaminated by Hydrocarbons. *Water Sci. Technol.* **2015**, *71*, 938–946. [CrossRef]
35. van Afferden, M.; Rahman, K.Z.; Mosig, P.; De Biase, C.; Thullner, M.; Oswald, S.E.; Müller, R.A. Remediation of Groundwater Contaminated with MTBE and Benzene: The Potential of Vertical-Flow Soil Filter Systems. *Water Res.* **2011**, *45*, 5063–5074. [CrossRef]
36. Rahim, F.; Abdullah, S.R.S.; Abu Hasan, H.; Kurniawan, S.B.; Mamat, A.; Yusof, K.A.; Ambak, K.I. A Feasibility Study for the Treatment of 1,2-Dichloroethane-Contaminated Groundwater Using Reedbed System and Assessment of Its Natural Attenuation. *Sci. Total Environ.* **2022**, *814*, 152799. [CrossRef]
37. *German Standard DWA-A 262*; Grundsätze für Bemessung, Bau und Betrieb von Kläranlagen mit bepflanzten und unbepflanzten Filtern zur Reinigung häuslichen und kommunalen Abwassers (DWA Principles for Dimensioning, Construction and Operation of Wastewater Treatment Plants with Planted and Unplanted Filters for Treatment of Domestic and Municipal Wastewater); DWA (Ed.) German Association for Water, Wastewater and Waste (DWA): Hennef, Germany, 2017; ISBN 978-3-88721-547-7.
38. Nivala, J.; van Afferden, M.; Hasselbach, R.; Langergraber, G.; Molle, P.; Rustige, H.; Nowak, J. The New German Standard on Constructed Wetland Systems for Treatment of Domestic and Municipal Wastewater. *Water Sci. Technol.* **2018**, *78*, 2414–2426. [CrossRef]
39. Czjzek, M.; Santos, J.-P.D.; Pommier, J. Crystal Structure of Oxidized Trimethylamine N-Oxide Reductase from Shewanella Massilia at 2.5 AÊ Resolution. *J. Mol. Biol.* **1998**, *284*, 435–447. [CrossRef]
40. Eberhardt, J.; Santos-Martins, D.; Tillack, A.F.; Forli, S. AutoDock Vina 1.2.0: New Docking Methods, Expanded Force Field, and Python Bindings. *J. Chem. Inf. Model.* **2021**, *61*, 3891–3898. [CrossRef] [PubMed]
41. Trott, O.; Olson, A.J. AutoDock Vina: Improving the Speed and Accuracy of Docking with a New Scoring Function, Efficient Optimization, and Multithreading. *J. Comput. Chem.* **2010**, *31*, 455–461. [CrossRef]
42. Reifferscheid, G.; Dill, F.; Fieblinger, D.; Gminski, R.; Grummt, H.-J.; Hafner, C.; Hollert, H.; Kunz, S.; Rodrigo, G.; Stopper, H.; et al. Untersuchung von Abwasserproben auf Gentoxizität. (Measurement of Genotoxicity in Wastewater Samples—Results of a Collaborative Study on the in Vitro Micronucleus Test in the Context of Standardisation According to ISO). *Umweltwiss. Und Schadst. Forsch.* **2007**, *19*, 7–16. [CrossRef]
43. Sommaggio, L.R.D.; Mazzeo, D.E.C.; Pamplona-Silva, M.T.; Marin-Morales, M.A. Evaluation of the Potential Agricultural Use of Biostimulated Sewage Sludge Using Mammalian Cell Culture Assays. *Chemosphere* **2018**, *199*, 10–15. [CrossRef]
44. Kim, H.; Xue, X. Detection of Total Reactive Oxygen Species in Adherent Cells by 2′,7′-Dichlorodihydrofluorescein Diacetate Staining. *J. Vis. Exp.* **2020**, *2020*, e60682. [CrossRef]
45. Graumans, M.H.F.; van Hove, H.; Schirris, T.; Hoeben, W.F.L.M.; van Dael, M.F.P.; Anzion, R.B.M.; Russel, F.G.M.; Scheepers, P.T.J. Determination of Cytotoxicity Following Oxidative Treatment of Pharmaceutical Residues in Wastewater. *Chemosphere* **2022**, *303*, 135022. [CrossRef]
46. Badr, D.M.; Hafez, H.F.; Agha, A.M.; Shouman, S.A. The Combination of α-Tocopheryl Succinate and Sodium Selenite on Breast Cancer: A Merit or a Demerit? *Oxidative Med. Cell. Longev.* **2016**, *2016*, 4741694. [CrossRef]
47. Lanza-Jacoby, S.; Cheng, G. 3,3′-Diindolylmethane Enhances Apoptosis in Docetaxel-Treated Breast Cancer Cells by Generation of Reactive Oxygen Species. *Pharm. Biol.* **2018**, *56*, 407–414. [CrossRef]
48. Roesslein, M.; Hirsch, C.; Kaiser, J.-P.; Krug, H.; Wick, P. Comparability of in Vitro Tests for Bioactive Nanoparticles: A Common Assay to Detect Reactive Oxygen Species as an Example. *IJMS* **2013**, *14*, 24320–24337. [CrossRef] [PubMed]
49. Magdeburg, A.; Stalter, D.; Schlüsener, M.; Ternes, T.; Oehlmann, J. Evaluating the Efficiency of Advanced Wastewater Treatment: Target Analysis of Organic Contaminants and (Geno-)Toxicity Assessment Tell a Different Story. *Water Res.* **2014**, *50*, 35–47. [CrossRef] [PubMed]
50. McBride, G.B.; Tanner, C.C. Modelling Biofilm Nitrogen Transformations in Constructed Wetland Mesocosms with Fluctuating Water Levels. *Ecol. Eng.* **1999**, *14*, 93–106. [CrossRef]
51. Rao, P.S.C.; Jessup, R.E. Simulation of Nitrogen Dynamics in Flooded Soils. *Soil Sci.* **1984**, *138*, 54–62. [CrossRef]
52. Sikora, F.J.; Tong, Z.; Behrends, L.L.; Steinberg, S.L.; Coonrod, H.S. Ammonium Removal in Constructed Wetlands with Recirculating Subsurface Flow: Removal Rates and Mechanisms. *Water Sci. Technol.* **1995**, *32*, 193–202. [CrossRef]

53. Gamar-Nourani, L.; Blondeau, K.; Simonet, J.-M. Influence of Culture Conditions on Exopolysaccharide Production by Lactobacillus Rhamnosus Strain C83. *J. Appl. Microbiol.* **1998**, *85*, 664–672. [CrossRef]
54. McKinley, J.W.; Siegrist, R.L. Soil Clogging Genesis in Soil Treatment Units Used for Onsite Wastewater Reclamation: A Review. *Crit. Rev. Environ. Sci. Technol.* **2011**, *41*, 2186–2209. [CrossRef]
55. Nevo, Z.; Mitchell, R. Factors Affecting Biological Clogging of Sand Associated with Ground Water Recharge. *Water Res.* **1967**, *1*, 231–236. [CrossRef]
56. Rubol, S.; Freixa, A.; Carles-Brangarí, A.; Fernàndez-Garcia, D.; Romaní, A.M.; Sanchez-Vila, X. Connecting Bacterial Colonization to Physical and Biochemical Changes in a Sand Box Infiltration Experiment. *J. Hydrol.* **2014**, *517*, 317–327. [CrossRef]
57. Zhou, Y.; Luo, S.; Yu, B.; Zhang, T.; Li, J.; Zhang, Y. A Comparative Analysis for the Development and Recovery Processes of Different Types of Clogging in Lab-Scale Vertical Flow Constructed Wetlands. *Env. Sci. Pollut. Res.* **2018**, *25*, 24073–24083. [CrossRef]
58. Boutin, C.; Prost-Boucle, S. Vertical Flow Constructed Wetlands Subject to Load Variations: An Improved Design Methodology Connected to Outlet Quality Objectives. *Water Sci. Technol.* **2015**, *72*, 817–823. [CrossRef]
59. Veeranagouda, Y.; Emmanuel Paul, P.V.; Gorla, P.; Siddavattam, D.; Karegoudar, T.B. Complete Mineralisation of Dimethylformamide by Ochrobactrum Sp. DGVK1 Isolated from the Soil Samples Collected from the Coalmine Leftovers. *Appl. Microbiol. Biotechnol.* **2006**, *71*, 369–375. [CrossRef] [PubMed]
60. Sanjeev Kumar, S.; Kumar, M.S.; Siddavattam, D.; Karegoudar, T.B. Generation of Continuous Packed Bed Reactor with PVA–Alginate Blend Immobilized Ochrobactrum Sp. DGVK1 Cells for Effective Removal of N,N-Dimethylformamide from Industrial Effluents. *J. Hazard. Mater.* **2012**, *199–200*, 58–63. [CrossRef] [PubMed]
61. Wang, J.; Liu, X.; Jiang, X.; Zhang, L.; Hou, C.; Su, G.; Wang, L.; Mu, Y.; Shen, J. Facilitated Bio-Mineralization of N,N-Dimethylformamide in Anoxic Denitrification System: Long-Term Performance and Biological Mechanism. *Water Res.* **2020**, *186*, 116306. [CrossRef]
62. Chudoba, J.; Zeis, K. Kinetics of Oxidation of Lower Aliphatic Amines and Pyridine Derivatives by the Dichromate Method. *Acta Hydrochim. Hydrobiol.* **1975**, *3*, 275–282. [CrossRef]
63. Janicke, W. *Chemische Oxidierbarkeit organischer Wasserinhaltsstoffe (Chemical Oxidizability of Organic Water Components)*; WaBoLu-Berichte, Berichtsreihe des Bundesgesundheitsamtes (Report series of the German Federal Health Agency); Dietrich Reimer Verlag: Berlin, Germany, 1983; ISBN 3-496-02164-0.
64. Anderson, J.E.; Mueller, S.A.; Kim, B.R. Incomplete Oxidation of Ethylenediaminetetraacetic Acid in Chemical Oxygen Demand Analysis. *Water Environ. Res.* **2007**, *79*, 1043–1049. [CrossRef] [PubMed]
65. Kim, Y.-C.; Sasaki, S.; Yano, K.; Ikebukuro, K.; Hashimoto, K.; Karube, I. Relationship between Theoretical Oxygen Demand and Photocatalytic Chemical Oxygen Demand for Specific Classes of Organic Chemicals. *Analyst* **2000**, *125*, 1915–1918. [CrossRef]
66. Balimandawa, M.; de Meester, C.; Léonard, A. The Mutagenicity of Nitrite in the Salmonella/Microsome Test System. *Mutat. Res. Genet. Toxicol.* **1994**, *321*, 7–11. [CrossRef] [PubMed]
67. Reifferscheid, G.; Ziemann, C.; Fieblinger, D.; Dill, F.; Gminski, R.; Grummt, H.-J.; Hafner, C.; Hollert, H.; Kunz, S.; Rodrigo, G.; et al. Measurement of Genotoxicity in Wastewater Samples with the in Vitro Micronucleus Test—Results of a Round-Robin Study in the Context of Standardisation According to ISO. *Mutat. Res. Genet. Toxicol. Environ. Mutagen.* **2008**, *649*, 15–27. [CrossRef]
68. Finlayson, K.A.; van de Merwe, J.P.; Leusch, F.D.L. Review of Ecologically Relevant in Vitro Bioassays to Supplement Current in Vivo Tests for Whole Effluent Toxicity Testing—Part 2: Non-Apical Endpoints. *Sci. Total Environ.* **2022**, *851*, 158094. [CrossRef]
69. Kuo, B.; Beal, M.A.; Wills, J.W.; White, P.A.; Marchetti, F.; Nong, A.; Barton-Maclaren, T.S.; Houck, K.; Yauk, C.L. Comprehensive Interpretation of in Vitro Micronucleus Test Results for 292 Chemicals: From Hazard Identification to Risk Assessment Application. *Arch. Toxicol.* **2022**, *96*, 2067–2085. [CrossRef] [PubMed]
70. Tarpey, M.M.; Wink, D.A.; Grisham, M.B. Methods for Detection of Reactive Metabolites of Oxygen and Nitrogen: In Vitro and in Vivo Considerations. *Am. J. Physiol. Regul. Integr. Comp. Physiol.* **2004**, *286*, R431–R444. [CrossRef] [PubMed]
71. Eckenfelder, W.W.; Ford, D.L.; Englande, A.J. *Industrial Water Quality*, 4th ed.; McGraw-Hill: New York, NY, USA, 2009; ISBN 978-0-07-154866-3.
72. Water Environment Federation (Ed.) *Operation of Municipal Wastewater Treatment Plants*, 6th ed.; Manual of practice No. 11; WEF Press; McGraw Hill: New York, NY, USA, 2008; ISBN 978-0-07-154367-5.